Bioorganic & Medicinal Chemistry 22 (2014) 6595–6615

Contents lists available at ScienceDirect

Bioorganic & Medicinal Chemistry

journal homepage: www.elsevier.com/locate/bmc

Vinylated linear P2 pyrimidinyloxyphenylglycine based inhibitors of the HCV NS3/4A protease and corresponding macrocycles

Anna Lampa [a], Hiba Alogheli [a], Angelica E. Ehrenberg [b], Eva Åkerblom [a], Richard Svensson [c,d], Per Artursson [c,d], U. Helena Danielson [b], Anders Karlén [a], Anja Sandström [a,*]

[a] Department of Medicinal Chemistry, Organic Pharmaceutical Chemistry, Uppsala University, BMC, Box 574, SE-751 23 Uppsala, Sweden
[b] Department of Chemistry-BMC, Uppsala University, BMC, Box 576, SE-751 23 Uppsala, Sweden
[c] Department of Pharmacy, Uppsala University, Box 580, SE-751 23 Uppsala, Sweden
[d] The Uppsala University Drug Optimization and Pharmaceutical Profiling Platform, Uppsala University, A Node of the Chemical Biology Consortium Sweden (CBCS), Box 580, SE-751 23 Uppsala, Sweden

ARTICLE INFO

Article history:
Received 15 July 2014
Revised 4 October 2014
Accepted 9 October 2014
Available online 18 October 2014

Keywords:
HCV
NS3
Protease inhibitors
Macrocyclization
Phenylglycine
Metathesis

ABSTRACT

With three recent market approvals and several inhibitors in advanced stages of development, the hepatitis C virus (HCV) NS3/4A protease represents a successful target for antiviral therapy against hepatitis C. As a consequence of dealing with viral diseases in general, there are concerns related to the emergence of drug resistant strains which calls for development of inhibitors with an alternative binding-mode than the existing highly optimized ones. We have previously reported on the use of phenylglycine as an alternative P2 residue in HCV NS3/4A protease inhibitors. Herein, we present the synthesis, structure–activity relationships and in vitro pharmacokinetic characterization of a diverse series of linear and macrocyclic P2 pyrimidinyloxyphenylglycine based inhibitors. With access to vinyl substituents in P3, P2 and P1′ positions an initial probing of macrocyclization between different positions, using ring-closing metathesis (RCM) could be performed, after addressing some synthetic challenges. Biochemical results from the wild type enzyme and drug resistant variants (e.g., R155 K) indicate that P3–P1′ macrocyclization, leaving the P2 substituent in a flexible mode, is a promising approach. Additionally, the study demonstrates that phenylglycine based inhibitors benefit from *p*-phenylpyrimidinyloxy and *m*-vinyl groups as well as from the combination with an aromatic P1 motif with alkenylic P1′ elongations. In fact, linear P2–P1′ spanning intermediate compounds based on these fragments were found to display promising inhibitory potencies and drug like properties.

1. Introduction

Hepatitis C is a major global health issue with an estimated global prevalence of ca. 2.2% and 350 000 related deaths every year.[1] The causative agent of the disease is the hepatitis C virus (HCV). The virus infects the liver, and can cause acute and chronic liver disease. HCV constitutes a major reason for liver transplantations in the western world.[2] The mainstay treatment has for long been based on the immunomodulating pegylated interferon-α alongside the broad-spectrum antiviral agent ribavirin. The treatment could progress up to 72 weeks and is associated with severe side-effects such as pancytomia, depression and flu-like symptoms.[3] Moreover, the success rate of the treatment is highly dependent on the viral genotype (i.e., genotype 1–6) with a success rate of ca. 45–50% for the prevalent genotype 1.[4] The significance of the disease and poor treatment options have made HCV a prioritized research area within the pharmaceutical industries the last decades, and from which results now are starting to be seen. In 2012 two direct acting antiviral drugs (DAAs), the protease inhibitors boceprevir[5] (Victrelis™, Merck & Co.) and telaprevir[6] (Incivek™,Vertex) were approved for the treatment of genotype 1, thus resulting in a significant better cure rate in combination with the standard therapy (up to 80%) and shortened treatment periods.[7] In 2013 two more DAAs, simeprevir,[8] a protease inhibitor, and sofosbuvir,[9] a polymerase inhibitor, were launched. In addition, several DAAs are currently in advanced clinical stages and these are evaluated in various combinations, including interferon-free alternatives. The treatment alternatives for HCV patients are definitely improving. However, the choice of treatment for a particular patient is complex, depending on several individual and viral factors such as genotype, subtype, disease progress, treatment history, tolerability etc., as

* Corresponding author. Tel.: +46 18 471 42 85; fax: +46 18 471 4474.
E-mail address: anja.sandstrom@orgfarm.uu.se (A. Sandström).

http://dx.doi.org/10.1016/j.bmc.2014.10.010
0968-0896/

well as cost. Besides, the efficacy of these medications can be hampered by emergence of drug resistance and more seriously cross resistance, as indicated in cell-based as well as clinical studies.[10,11] Thus, efforts to design and develop coming generation of DAAs that retain activity against resistant variants must be taken into consideration.

The genome of HCV contains single-stranded (+)-RNA that is translated into a polyprotein of approximately 3000 amino acids. The polyprotein consists of 10 viral proteins. The first third of the N-terminal part of the polyprotein encodes the structural region consisting of proteins C, E1, E2, and p7 which are involved in the structural build-up of the virion. The rest of the polyprotein encodes for the non-structural proteins NS2, NS3, NS4A, NS4B, NS5A and NS5B, which are essential in the viral replication machinery.[12,13] NS3 is a bifunctional enzyme containing a serine protease domain and a RNA helicase domain.[14] The NS3 protease is, when combined with its cofactor NS4A, responsible for deliberating the proteins NS4A, NS4B, NS5A and NS5B from the polyprotein. Several targets are explored for anti-HCV therapy, and the NS3/4A protease, along with NS5B polymerase, are among the more well-studied and promising considering its central role in the viral replication machinery. Moreover, the NS3 protease is involved in interference with the infected cell's natural antiviral response, thereby facilitating an evasion of the immune system for the virus.[15]

A specific characteristic of the NS3 protease is that it is inhibited by its own cleavage products.[16,17] Since this discovery, several so-called product-based HCV NS3/4A protease inhibitors have been developed.[18] The product-based inhibitors are characterized by an acidic functionality,[19] most often a carboxylic acid or an acylsulfonamide[20] in the C-terminal (Fig. 1). Another class of HCV NS3/4A protease inhibitors, the so-called electrophilic inhibitors utilizes an electrophilic functionality to interact covalently, and reversibly with the serine residue of the protease.[21] Proof-of-concept was established with ciluprevir, BILN-2061. This was the first NS3/4A protease inhibitor to show reduced HCV RNA levels in humans after oral administration.[22] Unfortunately, the development of ciluprevir was halted due to cardiotoxicity.[23,24] After ciluprevir, several NS3/4A protease inhibitors have entered clinical trials, all showing excellent inhibitory potencies (Fig. 1).

The main structural variations of the clinical candidates are the product-based or electrophilic functionality and if they are linear or macrocyclized between different positions. A consequence of the development of direct-acting antiviral HCV NS3/4A protease inhibitors is the possible emergence of resistant mutants which is a common setback among viral diseases in general. In vitro and in vivo studies have revealed mutations leading to protease variants with amino acid substitutions particularly in areas which interact with the P2 region of the protease inhibitor, both in the product-based and electrophilic class of inhibitors.[10,11,28,29] A common attribute among the inhibitors that have entered clinical trials so far, is that they carry a proline or proline mimic in the P2 position, the latter in the case of simeprevir (Fig. 1). These proline-based inhibitors are highly optimized and outstanding regarding antiviral efficacy. As an alternative to proline, we have previously presented inhibitors holding a phenylglycine (Phg) in the P2 position.[30–32] This inhibitor class has a different binding-conformation than proline-based inhibitors[30] and is therefore less affected by mutations that emerge in the presence of proline-based inhibitors.[33,34] In an attempt to optimize phenylglycine-based inhibitors, we have previously found that alkenylic elongations at the acylsulfonamide were more beneficial in phenylglycine-based inhibitors than proline-based inhibitors (A and B, Fig. 2). It was also found that the commonly utilized P1-residues norvaline, or vinyl cyclopropyl carboxylic acid (vinyl ACCA)[35] were not beneficial in combination with P2 phenylglycine.[30,31] However, incorporation of an aromatic P1 residue was more suitable (D, Fig. 2), and seems to be an interesting optimization point for phenylglycine-based inhibitors.[34] This leads us to believe that there are still many unraveled points for potentiation of phenylglycine-based inhibitors.

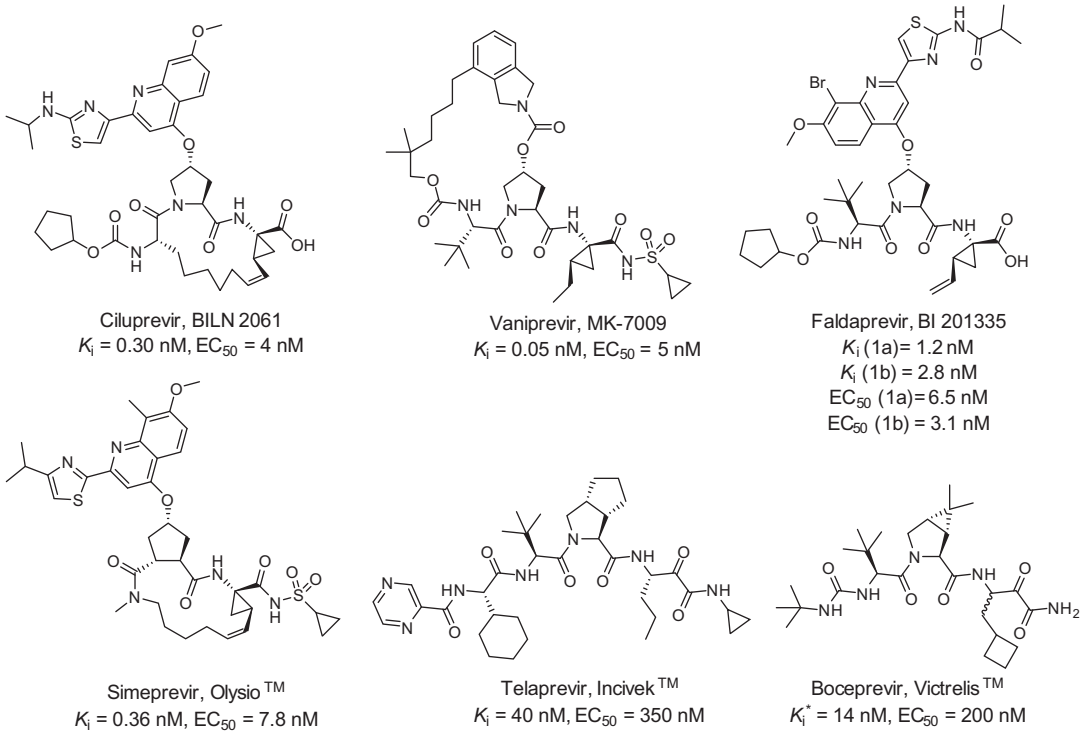

Figure 1. A selection of macrocyclic and linear product-based, and electrophilic HCV NS3/4A protease inhibitors that have entered clinical trials. Ciluprevir,[22] vaniprevir,[25,26] faldaprevir,[27] simeprevir,[8] telaprevir,[6] and boceprevir.[5]

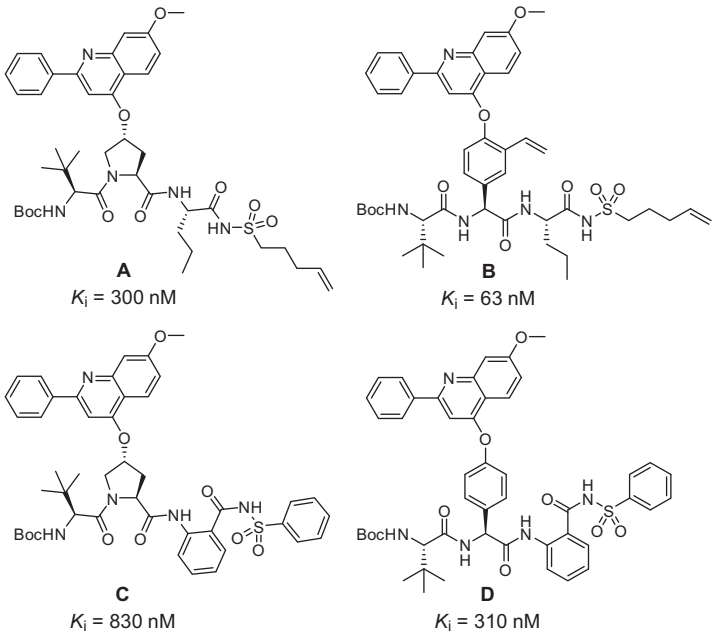

Figure 2. Two examples of fragments better suited with phenylglycine than proline. (1) Alkenylic P1′ elongations (**B** vs **A**); (2) aromatic P1 moiety (**D** vs **C**).

In a previous attempt to pin down the binding mode of phenylglycine-based inhibitors, we introduced conformational strain by macrocyclization between the P1′ and P2 positions. Disappointingly, potentiation of the inhibitory activity was only found in one case compared to the acyclic analogues possibly explained by a disruption of a beneficial π–π interaction between phenylglycine and H57 of the protease, caused by macrocyclization.[32] Also, the synthesis of the P2 building block containing a quinolinyloxy-type of substitution[36] on the phenylglycine was difficult and very slow. Thus, we were encouraged to find alternatives to the quinolinyloxy P2 substituent and combine this new alternative with the advantageous alkenylic acylsulfonamides and the aromatic P1 moieties. The 2-phenyl-4-methoxy-pyrimidinyloxy substituent was chosen as an interesting candidate for a P2 substituent.[37] The synthesis of the pyrimidine based P2 substituent opened up for diversification of the P2 substituent such as vinyl functionalities, inviting to macrocyclization to the P2 substituent from P3, which is an interesting option for macrocyclization.[38] Furthermore, by the use of alkenylic P1′ substituents, macrocyclizations connecting P1′ with the P3, as well as with the P2 substituent were interesting options. Indeed, modeling suggested a proximity between P3 and the alkenylic P1′ which motivated us to explore such a macrocyclization. We hoped that access to these different alternatives, as summarized in Figure 3, would provide us with a better understanding of the binding mode of phenylglycine-based inhibitors. Herein, we present the synthesis, structure–activity relationships and in vitro pharmacokinetic characterization for a diverse series of linear and macrocyclic HCV NS3/4A protease inhibitors.

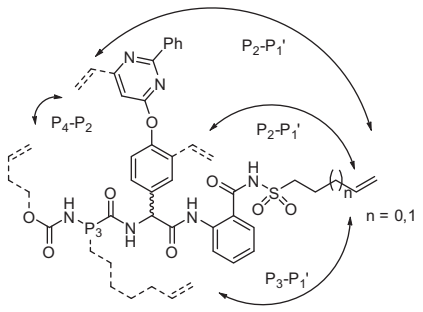

Figure 3. Summarized view of the different macrocyclization alternatives covered in this study.

2. Chemistry

The different P1–P1′ building blocks, shown in Scheme 1, were synthesized by coupling commercially available Boc-L-Nva, 2-(*t*-butoxycarbonylamino)benzoic acid (Boc-Abz-OH) with but-3-ene-1-sulfonamide[39] or pent-4-ene-1-sulfonamide,[39] using carbonyldiimidazole (CDI) and 1,8-diazabicycloundecene (DBU) in THF. CDI activation of the acid was performed under 60 °C for 1 h before addition of sulfonamide and DBU. Purification on silica gel removed traces of unreacted acid. This was followed by purification on aluminium oxide to remove any of the remaining sulfonamide. Building blocks **1**–**3** were obtained in a yield of 59–80% (Scheme 1).

The new P2 building block with a pyrimidine substituent was synthesized according to Scheme 2. To attain the P2-substituent containing a methoxy group in the 6-position of the pyrimidine, commercially available fenclorim needed reflux with sodium methoxide in methanol, contrary to a previously published synthesis in room temperature[40] After 7 h of reflux, the disubstituted byproduct (4,6-dimethoxy-2-phenylpyrimidin) started to be

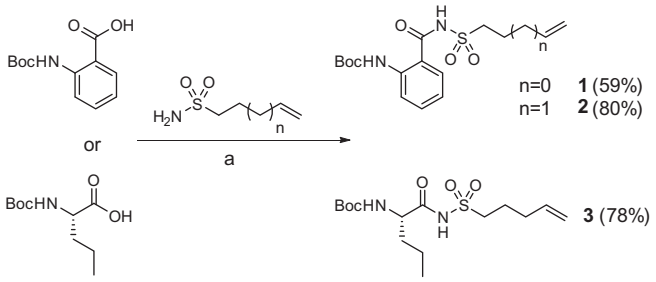

Scheme 1. Reagents: (a) CDI, DBU, THF, 60 °C → rt.

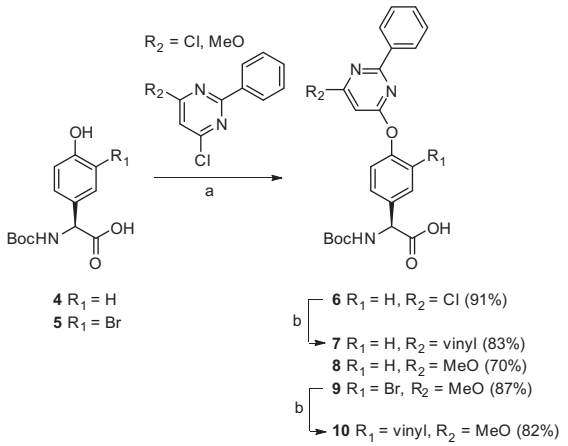

Scheme 2. Reagents: (a) KO*t*Bu, DMSO, rt. (R_2 = Cl)/64 °C (R_2 = OMe); (b) 2,4,6-trivinylcycloboroxane pyridine complex, $Pd(OAc)_2$, $[(tBu)_3PH]BF_4$, K_2CO_3, DME, H_2O, MW, 100 °C, 15 min.

formed and the reaction was interrupted. After extraction, 4-chloro-6-methoxy-2-phenylpyrimidine was obtained and characterized.

Starting with the Boc-protected 4-hydroxy-L-phenylglycine (**4**),[41] or the Boc-protected 3-bromo-4-hydroxy-L-phenylglycine (**5**),[42] the P2 building blocks **6**, **8** and **9** were synthesized through a nucleophilic aromatic substitution reaction using commercially available fenclorim or 4-chloro-6-methoxy-2-phenylpyrimidine together with potassium-*tert*-butoxide in DMSO at either 64 °C (**8** and **9**), or room temperature (**6**). Completion of the reactions was established by LC–MS and P2 building blocks **6**, **8** and **9** were obtained in 91%, 70%, and 87% yield, respectively. A microwave assisted Suzuki reaction using **6**, 2,4,6-trivinylcyclotriboroxane pyridine complex, and $[(tBu)_3PH]BF_4$ (Fu salt),[43] $Pd(OAc)_2$ in DME produced **7** in only 15 min at 100 °C and in a yield of 83% after precipitation. Compound **10** was generated through the same microwave assisted Suzuki reaction as **7** in a yield of 82%.

Synthesis of the P2–P1–P1′ compounds **11**–**15** (Scheme 3) were performed by peptide coupling of P2 building blocks **7**, **8** or **10** with the N-deprotected HCl-salts of **1**, **2** or **3** using *N*-[(dimethylamino)-1*H*-1,2,3-triazolo-[4,5-*b*]pyridine-1-yl-methylene]-*N*-methylmethanaminium hexafluorophosphate *N*-oxide (HATU) and diisopropylethylamine (DIEA). The P1–P1′ building blocks comprising an aromatic moiety (**1** and **2**) were coupled in dry DCM at 45 °C, while the coupling of the norvaline containing building block (**3**) was performed in dry DMF at room temperature After silica gel purification, compounds **11**–**15** were obtained in a yield of 18–96%. For the further coupling of **12**, the N-deprotection had to be performed using TFA in DCM, since the alternative deprotection using HCl/dioxane resulted in addition of HCl over the pyrimidine vinyl. The TFA-salt of **12** was coupled with *N*-[(But-3-en-1-yloxy)carbonyl]-3-methyl-L-valine, prepared according to a published patent,[44] using HATU in DMF resulting in **16** that was further purified by HPLC. Compound **13** was coupled both with Boc-2-amino-8 nonenoic acid and Boc-L-*t*Leu to generate **17** and **18** in 79% and 35% yield, respectively. The coupling of **15** with Boc-L-*t*Leu resulted in both diastereomers **19L** and **19D** in a yield of 15% and 10%, respectively.

Peptide coupling in the synthesis of phenylglycine-based inhibitors is normally performed in a fashion to retain the Boc-protecting group on the phenylglycine as long as possible throughout the synthesis; which is demonstrated and exemplified in Scheme 3. This is to avoid racemization on the phenylglycine α-carbon.[45] In the case of linear compounds **22** encompassing three vinyl groups (of which the corresponding P4–P2 cyclized variants will be prepared, vide infra), another approach was attempted to generate an intermediate useful in both the synthesis of linear and cyclized variants and also since we were interested in both epimers. Thus, compound **7** was coupled directly with the P3 building block, *N*-[(but-3-en-1-yloxy)carbonyl]-3-methyl-L-valine,[44] for further coupling with the P1–P1′ building block (Scheme 4). To enable this, **7** was first transformed into the methyl ester **20** (56%), under mild conditions using methyl iodide and cesium carbonate in DMF.[46] This was followed by Boc-deprotection using TFA in CH_2Cl_2 to avoid addition of HCl to the pyrimidine vinyl and HATU mediated coupling in DMF to give P2–P4 fragment **21** in a 62% yield. Microwave assisted ester hydrolysis of **21** using potassium carbonate in acetonitrile and coupling with the N-deprotected HCl salt of **3** gave both diastereomers **22L** and **22D** in a yield of 6% and 3.5%, respectively. Unfortunately, it was observed during this last step of the synthesis that byproducts were formed, with masses indicating that the ester deprotected P4–P2 starting material is decomposed during activation.[30,45]

Access of a vinylated pyrimidine-based P2 substituent, and alkenylic P1–P1′ building blocks invited to a new P2–P1′ macrocyclization connecting the pyrimidine-based substituent with P1′. A similar macrocyclization connecting the P2 substituent with P1′ has been investigated in a recent patent application.[47] The ring-closing metathesis reactions forming macrocycles connecting the P2 pyrimidine substituent and P1′ side chains are outlined in Scheme 5. Diolefinic compounds **11** and **12** were treated with Hoveyda–Grubbs 2nd generation catalyst in trifluorotoluene under microwave irradiation to obtain macrocycles **23** and **24** (Scheme 5). During the ring closure of **11** and **12**, a precipitate, most probably dimeric and polymeric starting material was formed apart from the desired product. The precipitation was more pronounced in the ring-closure of **12**, leading us to believe that the ring-closure of a compound containing an aromatic P1 moiety is more difficult than with a non-aromatic P1. After silica purification, compounds **23** and **24** were obtained in a 43% and 11% yield, respectively, in *trans* configuration only. Further coupling of **23** with Boc-L-*t*Leu yielded the P2–P1′ macrocyclic inhibitor **26** in a yield of 61%. The same coupling of **24** produced the P2–P1′ macrocyclic inhibitor **27** in a 20% yield.

Another type of P2–P1′ macrocyclization, is where the phenylglycine part of the P2 is connected with the alkenylic P1′ sidechain. A P2–P1′ type of cyclization has been reported before by us[32] and others.[48] The ring closure of **14** (Scheme 5) required a high (30 mol %) catalyst load before getting a satisfying amount converted starting material. Again, we experienced that ring-closure of **14**, with an aromatic P1 was complicated, leaving more unreacted linear starting material than ring-closure of compounds with norvaline P1.[32] Some dimeric and ring-contracted products were formed besides compound **25**, which was obtained in a 28% yield, in *cis* configuration. The P2–P1′ macrocyclic tripeptidic inhibitor **28** was obtained in a 33% yield by coupling **25** with Boc-L-*t*Leu.

The use of Boc-2-amino-8-nonenoic acid in P3 enabled ring-closure between P3 and P1′. P3–P1′ macrocycles have previously been investigated in P2 proline based inhibitors in a patent application.[49,50] The ring closure of **17** (Scheme 6) proved to be complicated. Full conversion of starting material was not obtained and large amounts of dimer, trimer, and ring-closed variants of the dimer and trimer were formed according to LC–MS. An interesting observation was made when a small fraction of **17** was purified on preparative HPLC with acetonitrile/water containing 0.05% formic acid as eluent, for biochemical evaluation. When comparing the ^{1}H NMR of **17**, purified on silica gel with **17**, purified on preparative HPLC, it was clear that the ^{1}H NMR were different; in particular the protons around the aromatic P1 moiety (Table 1). Thus, this indicates that **17** exists in two different conformations in where one of the conformations contains an internal hydrogen bond between the P1 amine hydrogen and the P1 carbonyl (Fig. 4), which would

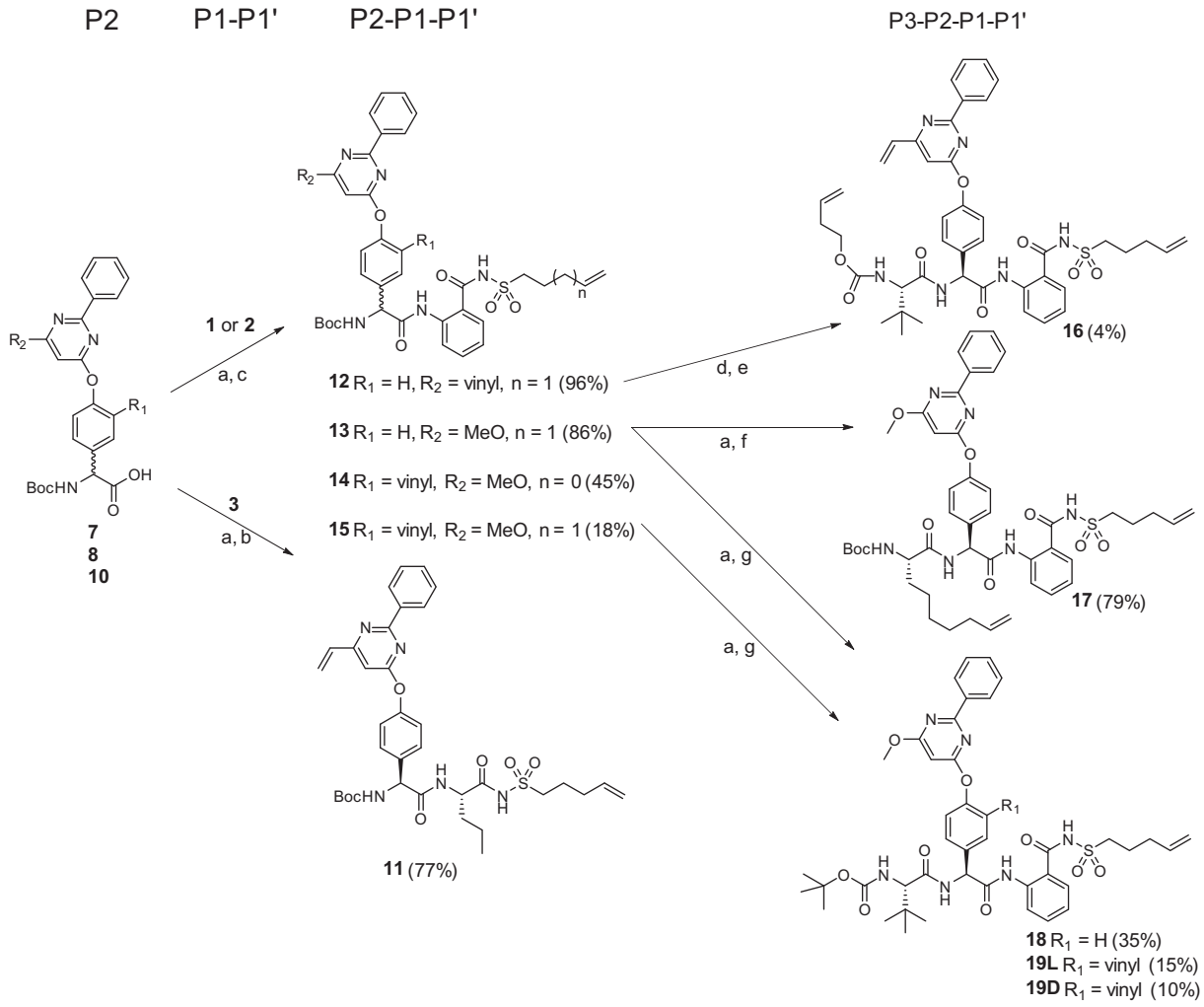

Scheme 3. Reagents: (a) 4.0 M HCl in dioxane; (b) HATU, DIEA, DMF, rt; (c) HATU, DIEA, DCM 45 °C; (d) TFA, DCM; (e) HATU, *N*-[(But-3-en-1-yloxy)carbonyl]-3-methyl-L-valine, DIEA, DMF, rt; (f) HATU, Boc-2-amino-8-nonenoic acid, 4-methylmorpholine, DMF; (g) HATU, Boc-L-*t*Leu, DIEA, DMF, rt.

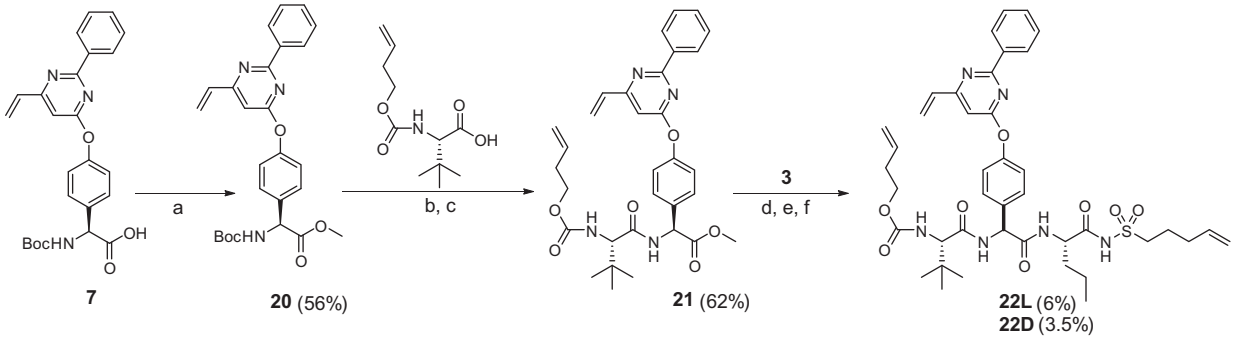

Scheme 4. Reagents: (a) $CsCO_3$, MeI, DMF; (b) TFA, DCM; (c) HATU, DIEA, DMF, rt; (d) K_2CO_3, MeCN, H_2O; (e) 4.0 M HCl in dioxane; (f) HATU, DIEA, DMF, rt.

create an unfavourable pose for ring-closure between P1′ and P3. In a previous publication it is shown that the proton next to the acetanilide (H_1 in Fig. 4) exhibit signals at unusually low field as an effect of the internal hydrogen bond.[51] The same observation was seen in the ^{1}H NMR of the two conformations of **17**; in the ^{1}H NMR from silica purified **17** H_1 resulted in a signal at a higher shift than in the corresponding HPLC (acidic eluent) purified **17**. This can be a result of that the internal hydrogen bond is weakened, or disrupted in the presence of acid. By adding formic acid to the reaction mixture during ring-closure of **17** it was evident from LC–MS that less dimerization and polymerization occurred and that the desired product **29** was the major product beside a small amount of ring-contracted product (**30**) (Fig. 5). After repeated purification on preparative HPLC the two diastereomers **29L** and **29D** could be isolated in 11% and 6% yield, respectively. Additionally, the ring contracted product **30** was isolated as a diastereomeric mixture in a yield of 3%. The mixed fractions from purification of **29** were pooled and subjected to reduction using

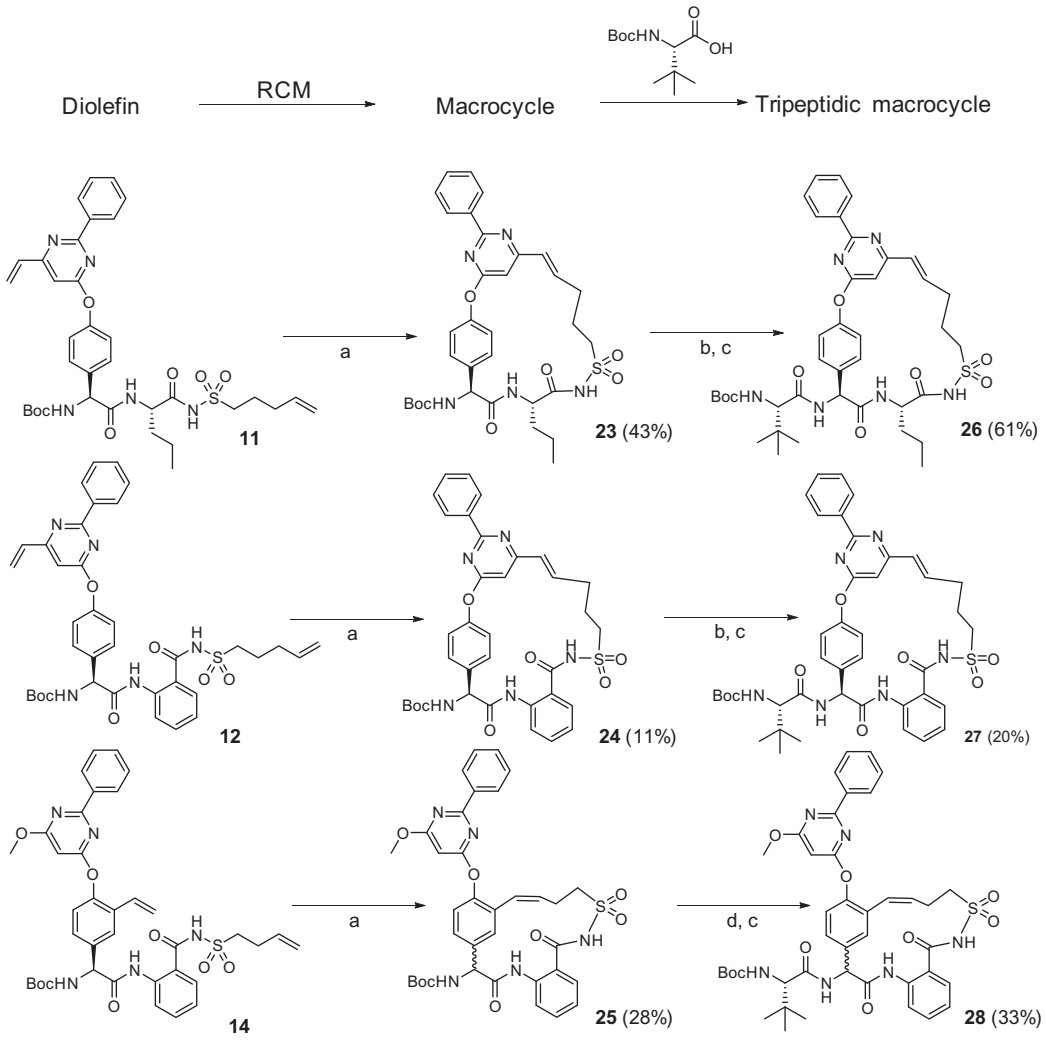

Scheme 5. Reagents: (a) Hoveyda–Grubbs 2nd generation catalyst, trifluorotoluene; (b) TFA, DCM; (c) HATU, Boc-L-*t*Leu, DIEA, DMF, rt; (d) 4.0 M HCl in dioxane.

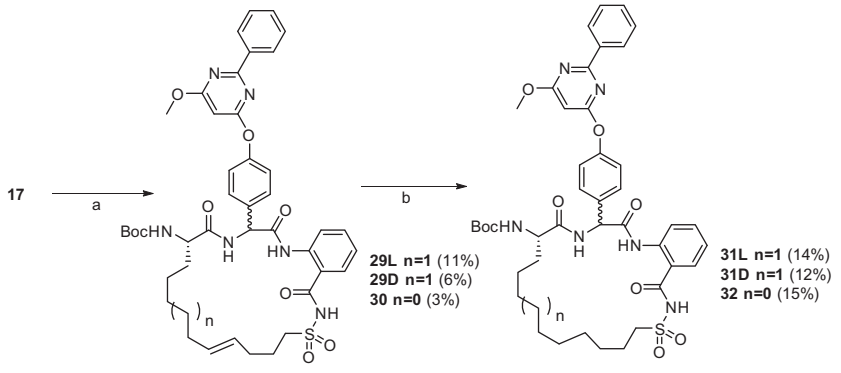

Scheme 6. Reagents: (a) Hoveyda–Grubbs 2nd generation catalyst, trifluorotoluene, formic acid; (b) Mixed fractions from purification of 29, H_2, Pd/C, THF.

H_2 and palladium on charcoal in methanol. After reduction and purification saturated inhibitors **31L**, **31D** and **32** were obtained in a yield of 14%, 12% and 15% (over the last step), respectively.

The use of *N*-[(but-3-en-1-yloxy)carbonyl]-3-methyl-L-valine in P3 also enabled P4–P2 macrocyclization. This cyclization is of the same type as in vaniprevir.[26] The ring-closure of **21** (Scheme 7) went rather smooth and without precipitation, although trace amounts of ring-contracted product and polymeric material were formed beside the main product **33** which was obtained in a yield of 68%. Ester hydrolysis of **33** followed by coupling with Boc deprotected **2** and **3** in the same inverse type of peptide synthesis as performed with compound **21**, resulted in P4–P2 macrocyclic inhibitors **34** and **35** in a respective yield of 45% and 32%. The decomposition of the P4–P2 building block that occurred for compound **21** was not observed in this case. We therefore believe that to avoid not only racemization, but also degradation, of the

Table 1
Variations in ^{1}H NMR shifts of H_1–H_4 of compound **17**, as a consequence of purification method used

	17 after silica purification	**17** after acidic HPLC purification
Proton	^{1}H NMR δ	^{1}H NMR δ
H_1	8.45	8.17
H_2	7.40	7.58
H_3	7.07	7.25
H_4	8.14	7.73

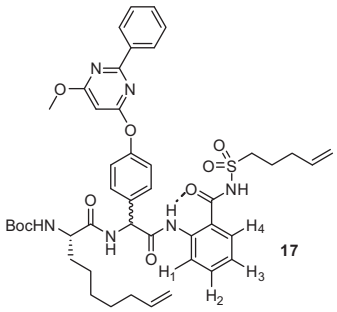

Figure 4. An internal hydrogen bond in compound **17** influencing the ^{1}H NMR shifts of H_1–H_4.

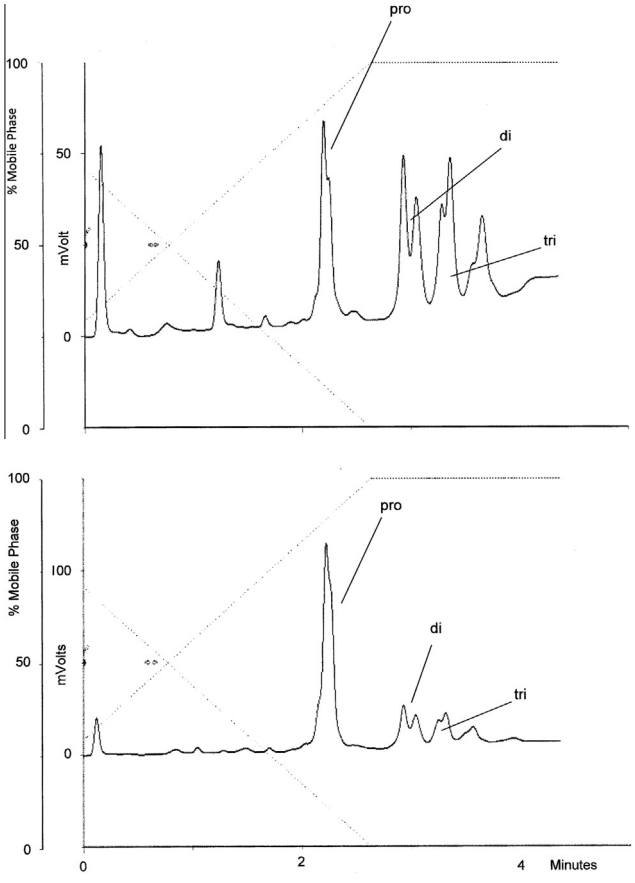

Figure 5. LC-UV chromatograms (254 nm) on crude products after ring-closure of **17** showing product (pro), dimers (di) and trimers (tri). Above: **17**, Hoveyda–Grubbs 2nd generation catalyst, trifluorotoluene, 100 °C, 5 min. Below: **17**, Hoveyda–Grubbs 2nd generation catalyst, formic acid, trifluorotoluene, 100 °C, 5 min.

phenylglycine-containing fragment it is necessary to keep the Boc-protecting group as long as possible throughout the synthesis, or to involve the N-terminal in a macrocycle which evidently protects the P4–P2 building-block from decomposition, but also from racemization since compounds **34** and **35** were only obtained as one diastereomer in *trans* conformation.

To evaluate the effectiveness of the new pyrimidine-based P2 substituent, the two reference analogues to compounds **19L** and **19D** containing a quinoline-based P2 substituent were synthesized (Scheme 8). Coupling of compound **36** [31] with the N-deprotected HCl salt of **2**, using HATU and DIEA in DCM and subsequent coupling with P3 Boc-L-*t*Leu and HPLC purification yielded compounds **38L** and **38D** in a yield of 10%, respectively.

3. Biochemical evaluation

The inhibitory effects (K_i-values) for compounds **12**–**19**, **22**, **25**–**32**, **34**–**35** and **38** were evaluated in a biochemical inhibition assay using full length NS3 protein from genotype 1a and a sixteen amino acid fragment, which corresponds to the activating region of NS4A (Scheme 8, and Tables 2–6).[52] Additionally, compound **29D** was evaluated with the drug resistant A156T, D168V and R155 K variants of the protease.[33] Inhibition constants were measured and vitality values (V) calculated (Table 7). Vitality values represent normalized inhibitory effects of the inhibitors with respect to the effects from amino acid substitutions on catalytic efficiency (k_{cat}/K_m) of the enzyme variants. A vitality value less than 1 demonstrates a more efficient inhibitor against the mutated variant compared to the wild type enzyme, while if $V > 1$ the inhibitor is less efficient against the mutated virus.[33] A mixture of compounds **19L** and **19D**, **38L** and **38D** and compound **29D** were also tested for EC_{50}-values using the Huh-7 cell line containing subgenomic HCV RNA genotype 1b replicon with firefly luciferase resulting $EC_{50} > 10$ μM (**19L** and **19D**), $EC_{50} = 5.4$ μM (**38L** and **38D**) and $EC_{50} = 15$ μM (**29D**).[53]

4. In silico and in vitro physicochemical and pharmacokinetic profiling

A few representative compounds (i.e., **13**, **15**, **17**, **18**, **19**, **29L** and **29D**) with good inhibition potencies were selected for in silico and in vitro physicochemical and pharmacokinetic profiling. The predicted pK_a and log$D_{7.4}$ values for compounds **13**, **15**, **17**, **18**, **19**, **29L** and **29D** were calculated using ADMET predictor v.5.5 and are presented in Table 8. The calculated pK_a-values span between 5.8 and 6.2 for the acidic acylsulfonamide group in the inhibitors and the corresponding log$D_{7.4}$-values between 3.5 and 4.8. From these log$D_{7.4}$ values low solubility, high permeability and a moderate to high metabolism would be expected.[54]

All compounds (**13**, **15**, **17**, **18**, **19**, **29L** and **29D**) showed a moderate (>20 μM) to good (>100 μM) solubility ranging from 33 μM to more than 100 μM; the latter exemplified by the truncated compounds **13** and **15** having solubilities close to or above 100 μM as this concentration is the limit of the assay. Metabolic stability was determined by incubating the compounds with pooled human liver microsomes. The in vitro half-life ($t_{1/2}$) and the in vitro intrinsic clearance (Cl_{int}) were calculated utilizing previously published models[55,56] and the results are presented in Table 8. The Cl_{int} primarily describes the compound sensitivity towards oxidative metabolism and can be used as a prediction of the in vivo Cl_{int} if the total clearance mechanism is mainly hepatic and when oxidative metabolism dominates. The cut-off values that were used to classify the compounds regarding metabolic stability are as follows: $Cl_{int} < 47$ (μl/min/mg) indicates a low risk for high first metabolism in vivo, $47 < Cl_{int} < 92$ a moderate risk, and $Cl_{int} > 92$ a high risk. All the linear inhibitors **13**, **15**, **17** and **18** showed a moderate risk of oxidative metabolism (Cl_{in} = 60–86 μL/min/mg),

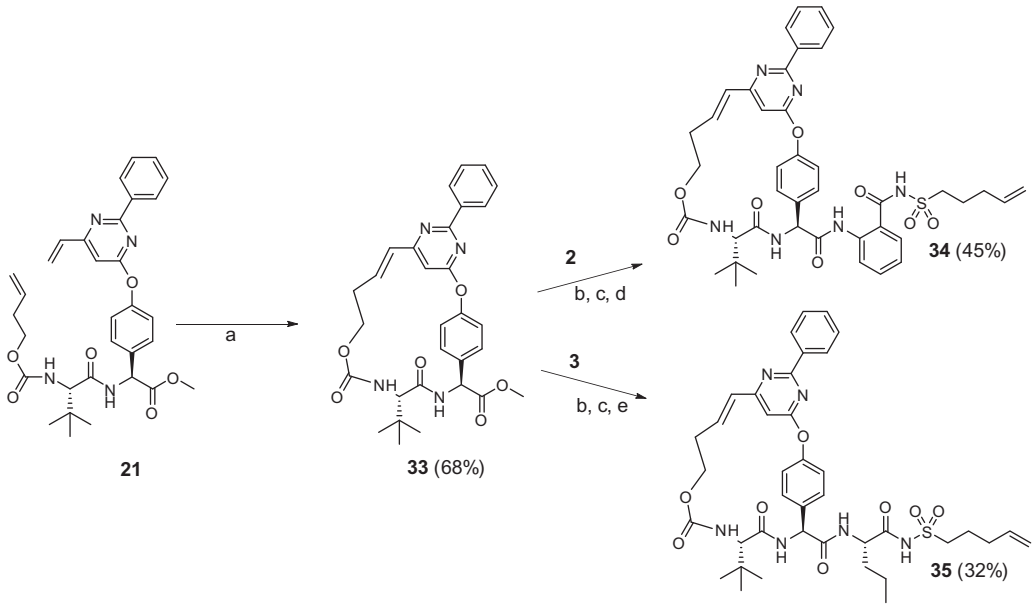

Scheme 7. Reagents: (a) Hoveyda–Grubbs 2nd generation catalyst, trifluorotoluene; (b) K_2CO_3, MeCN, H_2O (c) 4.0 M HCl in dioxane; (d) HATU, DIEA, DCM, 45 °C; (e) HATU, DIEA, DMF, rt.

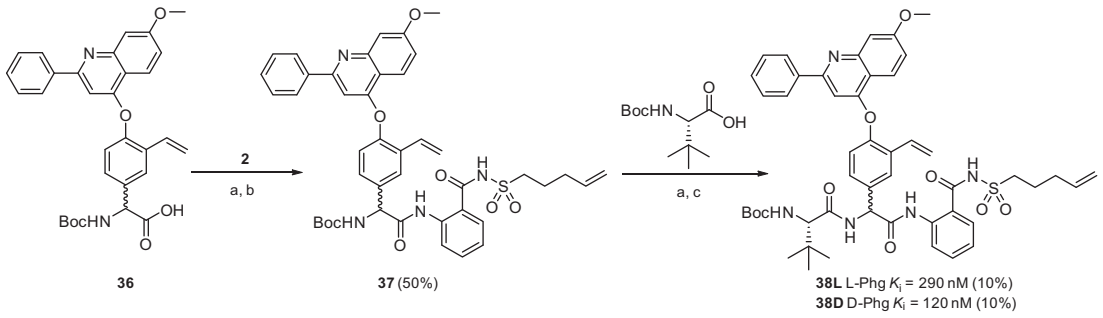

Scheme 8. Reagents: (a) 4.0 M HCl in dioxane; (b) HATU, DIEA, DCM, 45 °C; (c) HATU, DIEA, DMF, rt.

except for compound **19** (Cl_{in} = 17 μL/min/mg). The two macrocyclic compounds **29L** and **29D** proved to be moderate to highly susceptible for oxidative metabolism (Cl_{in} = 87 and 137 μL/min/mg, respectively). Prediction of the intestinal epithelial permeability, presented in Table 8, expressed as apparent permeability coefficients (P_{app}), for compounds **13**, **15**, **17**, **18**, **19** , **29L** and **29D**, were determined from transport rates across Caco-2 cell monolayers, as described previously.[57] However, a modified assay based on more physiological media had to be devised because all tested compounds displayed very strong adsorption to the plastic ware. Briefly, to minimize the nonspecific binding, fasted state simulated intestinal fluid (FASSIF)[58] was used in the apical (donor) compartment and a 1% (w/v) bovine serum albumin (BSA) solution of Hank's Buffered Salt Solution (HBSS)[59] was used in the basolateral (receiver) compartment. Using this format, the experiments could be run with reasonable mass balances above 64%. In our calibrated assay setup, a P_{app} value below 0.2×10^{-6} cm/s indicates low permeability, a P_{app} value between 0.2×10^{-6} cm/s to 1.6×10^{-6} cm/s indicates moderate permeability, and a P_{app} value above 1.6×10^{-6} cm/s indicates high permeability.[60] The truncated linear P2–P1′ spanning inhibitor **13** penetrated the intestinal epithelial cells very well ($P_{app} = 4.0 \times 10^{-6}$ cm/s). The remaining compounds had moderate to low permeability, for example, the macrocycles **29L** and **29D** displayed P_{app}-values of 0.22×10^{-6} and 0.15×10^{-6} cm/s, respectively.

5. Discussion

In an attempt to further depeptidize, optimize, and attain information about the binding-mode of P2 phenylglycine-based HCV NS3/4A protease inhibitors, we decided to combine a few previously discovered promising fragments for this type of inhibitors such as alkenylic P1′ elongations and aromatic P1 moieties.[31,61] Furthermore, the synthesis of the P2 building block was simplified and the reaction time was considerably shortened by introduction of a pyrimidine-based P2 substituent as compared to the previously used quinoline (see Fig. 2). Through the possibility of introducing vinyls on both the P2 phenylglycine part itself and on its pyrimidine substituent, and utilizing alkenylic substituents at the P3 and P1′ positions, macrocyclization could be performed between several positions in the molecules, which eventually opened up for an initial probing of the impact of different types of macrocycles in these inhibitors. Molecular modeling especially invited to some of the attempted macrocylizations. For example, modeling of compound **34** overlaid with vaniprevir showed that **34** occupies the same space, except for the phenyl substituent on the pyrimidine which sticks out into a pocket formed by the helicase. Though, both macrocycles show a good overlap and form the same backbone interactions with the protein (Fig. 6). Thus, this model motivated us to explore the P4–P2 cyclization. Modeling of compound **17** furthermore indicated a proximity between the

Table 2
Inhibitory potencies (K_i) of linear inhibitors measured with full-length NS3/4A protein from genotype **1a**

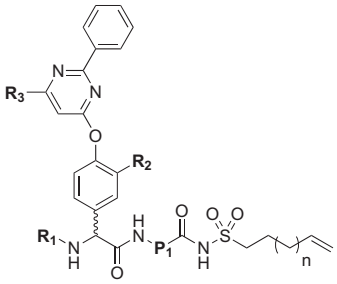

Compound	R_1	R_2	R_3	P1	n	$K_i \pm$ SD (μM)
12	Boc	H			1	0.22 ± 0.022
13	Boc	H			1	0.60 ± 0.14
14	Boc				0	0.37 ± 0.06
15	Boc				1	0.19 ± 0.02
16	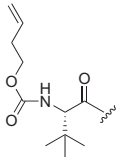	H			1	0.11 ± 0.011
17	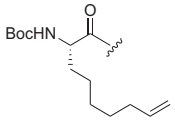	H			1	0.23 ± 0.03
18[a]	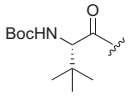	H			1	0.095 ± 0.013
19L	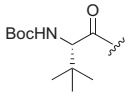				1	0.026 ± 0.0025
19D	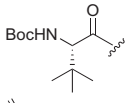				1	0.033 ± 0.0033
22L	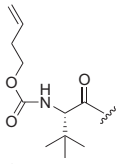	H			1	0.53 ± 0.09
22D	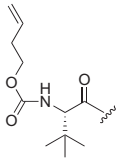	H			1	0.42 ± 0.06

SD, standard deviation. [a]Diasteromeric mixture L:D 5:2.

alkenylic P3 and P1′ substituents, with a distance that invites to macrocyclization. Modeling of **29L** shows that a macrocycle connecting P3 and P1′ can be accommodated by the protease and that it forms a distinct hydrophobic interaction with the side chain of Lys136 (Fig. 7).

The synthetic routes were designed to enable development of linear inhibitors as well as macrocyclic inhibitors connecting the P4–P2, P3–P1′ and P2–P1′ positions (Fig. 3). Our previous attempts of macrocyclizations using ring closing metathesis reactions (RCM) have proven to be highly substrate dependent. Thus, difficult

Table 3
Inhibitory potencies (K_i) of P2–P1′ macrocycles measured with full-length NS3/4A protein from genotype **1a**

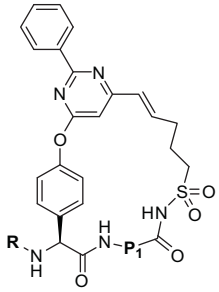

Compound	R	P1	Ring size	K_i ± SD (μM)
26	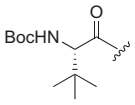		20	2.4 ± 0.3
27	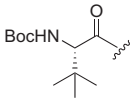		21	0.66 ± 0.22

SD, standard deviation.

Table 4
Inhibitory potencies (K_i) of P2–P1′ macrocyclic inhibitors measured with full-length NS3/4A protein from genotype **1a**

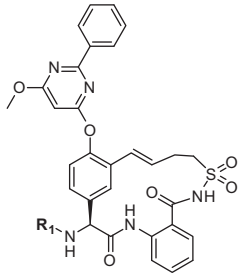

Compound	R_1	Ring size	K_i ± SD (μM)
25	Boc	15	1.3 ± 0.27
28	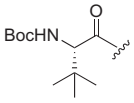	15	0.63 ± 0.14

SD, standard deviation.

substrates without a preorganized conformation that facilitates contact between the two vinyls, can be associated with the formation of side products such as the ones resulting from ring contraction and isomerization.[32] In this study another complicated factor arose through the introduction of a rigid ortho acylanilide type of P1–P1′ buildning block that retains an internal hydrogen bond. RCM between the P1–P1′ building block and the vinyl in P3 position was accompanied with side reactions and polymerization issues in particular. However, the outcome was found to be dramatically improved by the addition of acid that interrupted the internal hydrogen bond and thus improved flexibility of the molecule. In this context it could be worth mentioning that Grubbs and coworkers have observed that presence of acetic acid also could prevent undesirable isomerization during olefin metathesis.[62]

The inhibitory potencies of the linear and cyclic inhibitors produced in this study were evaluated and found to be in the range of

Table 5
Inhibitory potencies (K_i) of P3–P1′ macrocyclic inhibitors measured with full-length NS3/4A protein from genotype **1a**

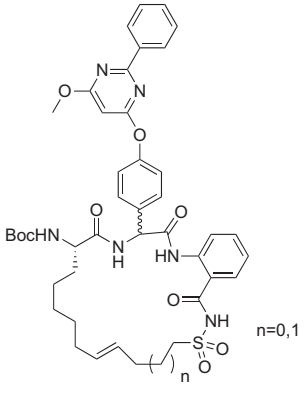

Compd	Ring size	K_i ± SD (μM)
29L	21	0.11 ± 0.02
29D	21	0.08 ± 0.009
30	20	0.22 ± 0.048
31L	21 saturated	0.11 ± 0.01
31D	21 saturated	0.11 ± 0.01
32	20 saturated	0.13 ± 0.02

SD, standard deviation.

Table 6
Inhibitory potencies (K_i) of P4–P2 macrocyclic inhibitors measured with full-length NS3/4A protein from genotype **1a**

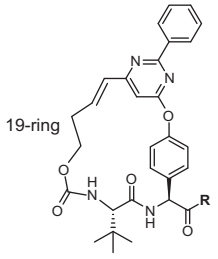

Compound	R	K_i ± SD (μM)
34	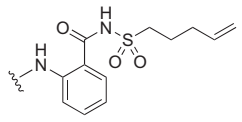	0.39 ± 0.08
35	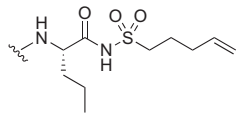	1.57 ± 0.29

SD, standard deviation.

26 nM to 1.6 μM. The inhibitory potencies of compounds **19L** and **19D** (K_i = 26 nM, and 33 nM), comprising the pyrimidine-based P2-substituent and aromatic P1 moiety, revealed that the new 2-phenyl-4-methoxy-pyrimidinyloxy P2 substituent was tolerated and led to more potent inhibitors compared to compounds **38L** and **38D** (K_i = 290 nM and 120 nM, Scheme 8), containing the quinoline-based P2 substituent. This improvement in inhibitory activity and the considerably simplified synthesis merit further use of the pyrimidine-based P2 substituent.

The combination of a P2 substituent based on pyrimidine with an aromatic P1 moiety was also revealed to be well-tolerated by the comparison of quinoline-substituted compound **B** with a norvaline

Table 7
Inhibition constants (K_i) and vitality values (V) evaluated with A156T, D168V, and R155K variants of full-length NS3/4A

Compound	A156T		D168V		R155K	
	K_i ± SD (nM)	*V*	K_i ± SD (nM)	*V*	K_i ± SD (nM)	*V*
29D	160	2.2	600	3.0	220	0.50

SD, standard deviation.
V, vitality values.[33]

in the P1 position (K_i = 63 nM), to compound **19L** (K_i = 26 nM). Thus, the choice of an aromatic P1 fragment seems as a promising alternative to norvaline. This was further strengthened when comparing the linear compounds, with a 2-phenyl-4-vinyl-pyrimidinyloxy P2 substituent and a P3 *N*-[(but-3-en-1-yloxy)carbonyl]-3-methyl-L-valine. Compound **16** (K_i = 110 nM), containing the aromatic P1 moiety is almost five times as potent as the norvaline containing compound **22L** (K_i = 530 nM). The differences between an aromatic P1 group and norvaline in P1 are also shown in the macrocyclic compounds. When comparing the P2–P1′ macrocyclic compound **27** (K_i = 660 nM), with an aromatic P1 residue to the norvaline containing analogue **26** (K_i = 2400 nM), a fourfold improvement in inhibitory potency is shown for the compound with an aromatic P1. The same fourfold difference is seen when comparing the P4–P2 macrocyclic compound **34** (K_i = 390 nM) containing an aromatic P1 with the norvaline analogue **35** (K_i = 1570 nM).

A beneficial π–π interaction between the vinyl substituent on the phenylglycine and the catalytic H57 has previously been proposed,[31,32] and this hypothesis is further strengthened herein. Thus, when comparing the P2 2-phenyl-4-methoxy-pyrimidinyloxy substituted P2–P1′spanning compounds **13** (K_i = 600 nM) and **15** (K_i = 190 nM), a threefold preference is seen for compound **15** that has a vinyl substituent on the phenylglycine ring. The same trend is seen when comparing the longer P3-P1′ spanning equivalents **18** (K_i = 95 nM) and **19L** (K_i = 26 nM), that yet again shows a threefold advantage for vinylated compound **19L**. An obvious drop in potency comes with the P2–P1′ ring-closure of the P2–P1′spanning compound **14** (K_i = 370 nM) into macrocyclic **25** (K_i = 1300 nM) as well as for the longer P3-P1′spanning compound **19L** (*K*i = 26 nM) and macrocyclic **28** (K_i = 630 nM). Thus, constraining the P2 vinyl and the alkenylic P1′ results in a less efficient inhibitors, which is in line with our previous observations.[32]

Another example of reduction in inhibitory activity after the alkenylic P1′ is constrained is seen for the linear P2–P1′ spanning compound **12** (K_i = 220 nM) with a 2-phenyl-4-vinyl-pyrimidinyloxy P2 substituent. After P2–P1′ macrocyclization, and now with the vinyl on the pyrimidine ring, and further coupling with P3 Boc-L-*t*Leu, the P3–P1′ spanning P2–P1′ macrocyclic compound **27** (K_i = 660 nM), shows a threefold drop in potency, even though it holds a P3 substituent.

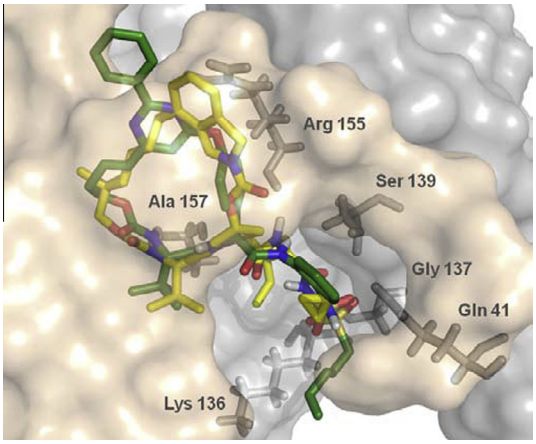

Figure 6. Overlay of compound **34** (green) and Vaniprevir (yellow) docked in the full-length NS3 protease binding site of the 1CU1 crystal structure.[14] The protease domain is shown in grey, the NS3 helicase domain is shown in beige.

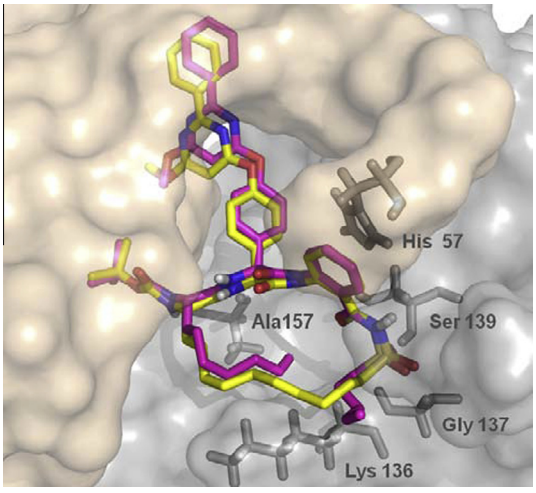

Figure 7. Overlay of acyclic compounds **17** (pink) and **29L** (yellow) docked in the full-length NS3 protease binding site of the 1CU1 crystal structure.[14] The protease domain is shown in grey, the NS3 helicase domain is shown in beige.

From modeling (Fig. 6), the macrocyclization connecting the P3 with the P2 substituent seemed very promising in line with vaniprevir. The biochemical evaluation was thus disappointing. Nevertheless, the P4–P2 macrocyclic inhibitors **34** (K_i = 390 nM), with an aromatic P1 residue, and **35** (K_i = 1570 nM), with norvaline in P1 position, showed a slightly better inhibitory potency than the corresponding P2-P1′ macrocyclic inhibitors **27** (K_i = 660 nM),

Table 8
Measured solubility, metabolic stability in human microsomes, and Caco-2 permeability of compounds **13**, **15**, **17**, **18**, **19**, **29L** and **29D**, and calculated acidic pK_a values (acyl sulfonamides), and log$D_{7.4}$-values

	In vitro				In silico	
			Metabolic stability			
Compd	Solubility (μM) pH 7.4	Caco-2 Permeability P_{app} (10^{-6} cm/s)[a] a-b[b]	Cl^c_{int} (μL/min/mg)	$t^d_{1/2}$ (min)	pK_a	Log$D_{7.4}$
13	93	4.0	86	16	5.8	3.5
15	101	1.0 ± 0.7	66	21	5.8	4.0
17	91	0.22 ± 0.2	60	23	6.0	4.8
18	33	0.22 ± 0.04	64	22	6.0	4.3
19[e]	66	1.7	17	83	6.0	4.7
29L	51	0.35 ± 0.12	87	16	6.2	4.0
29D	51	0.15 ± 0.11	137	10	6.2	4.0

[a]P_{app} = apparent permeability coefficient. [b]a–b = apical to basolateral. [c]Cl_{int} = in vitro clearance. [d]$t_{1/2}$ = in vitro half-life. [e]A mixture of **19L** and **19D**.

and **26** (K_i = 2400 nM). Again, the impairment caused by straining the alkenylic P1′ is shown.

As discussed above the P1′–P3 cyclization, which is overall poorly explored in HCV NS3/4A protease inhibitors, looked advantageous for the phenylglycine-based inhibitor **17** when it comes to molecular modelling (Fig. 7). Actually, biochemical evaluations of the formed macrocyclic products, that is, **29L** (K_i = 110 nM), **29D** (K_i = 80 nM), and ring contracted product **30** (K_i = 220 nM), reveal the first examples in this study of where ring-closure is slightly favored over the linear analogue **17** (K_i = 230 nM). **29D** was also found to retain decent potency on the A156T (K_i = 160 nM, V = 2.2) and D168V (K_i = 600 nM, V = 3.0) and R155 K (K_i = 220 nM, V = 0.50) mutants. The vitality value of 0.5 for the R155K variant; that is considered as one of the most serious drug resistant enzyme variants arising after treatment with DAAs,[10,63] is particularly worthy to note.

A driving force for the development of macrocycles in drug development are, besides a possible preorganization of bioactive conformation with positive entropic effect for the binding efficiency as a result, the pharmacokinetic advantages such as increased cell permeability and metabolic stability often associated with such compounds. Thus, to support further exploration of compounds derived from the promising macrocycles **29L**/**D** we were eager to see its in vitro pharmacokinetic characteristics. Unfortunately, both macrocycles proved to have poor pharmacokinetic properties as shown by high metabolic susceptibility and poor intestinal permeability (Table 8), which partly can explain the inhibitory efficiency drop to 15 μM (EC_{50}-value) for **29D** in the replicon assay.

In regard to the overall macrocyclic scan performed in this study it appears that macrocyclizations involving either the P2 substituent or the P2 phenylglycine part are damaging for inhibitory activity, and that P1′ to P3 macrocyclizations seem most promising to pursue in terms of inhibitory potency on wildtype and drug resistant strains of the enzyme. Thus, the importance of the retaining a flexible P2 side-chain in this type of inhibitors is established. The importance of flexible P2 substituents in retaining inhibitory potency for drug resistance enzyme variants has recently been proposed.[11]

What is particularly noteworthy in this study was that the intermediate compounds in synthesis, that is, the linear P2–P1′ spanning compounds with aromatic P1 residues, that is, **12** (K_i = 220 nM), **13** (K_i = 600 nM), **14** (K_i = 370 nM), and **15** (K_i = 190 - nM) retained impressive inhibitory potency without a P3 building block. Considering the smaller size combined with the good solubility and somewhat better intestinal permeability of compound **13** (solubility = 93 μM, $P_{app} = 4.0 \times 10^{-6}$ cm/s) and **15** (solubility = 101 μM, $P_{app} = 1.0 \times 10^{-6}$ cm/s) it seemed worthwhile to further explore the P2–P1′ spanning inhibitors with the 2-phenyl-4-methoxy-pyrimidinyloxy P2 substituent, a vinylated phenylglycine in P2, an aromatic P1 and alkenylic elongation in P1′.[64]

6. Conclusion

In summary, access to vinylated P3, P2 and P1 building blocks combined with a careful synthetic planning allowed preparation of a diverse set of RCM produced macrocycle-based HCV NS3/4A protease inhibitors and their corresponding linear analogues. Biochemical results proved that it is beneficial to substitute the P2 phenylglycine with *p*-phenylpyrimidinyloxy and *m*-vinyl groups. The inhibitors were further successfully combined with an aromatic P1 residue with alkenylic P1′ elongations, which eventually led to the discovery of truncated P2–P1′ based inhibitors with promising inhibitory potencies and in vitro pharmacokinetic properties. Probing of various macrocycles in P2 phenylglycine based inhibitors revealed that macrocyclizations involving either the P2 phenylglycine part or its *p*-pyrimidine substituent are detrimental for the inhibitory activities, which stresses the importance of having a flexible P2 moiety in this type of inhibitors. On the other hand, P1′ to P3 macrocyclization were allowed in terms of inhibitory potency on the wildtype and drug resistant strains of the enzyme, although further optimizations of this class of inhibitors are necessary to improve apparent intestinal permeability and metabolic stability. It is further shown herein that the RCM reactions which are hampered by internal hydrogen bonds could be made feasible by the addition of formic acid.

7. Experimental section

7.1. Chemistry

Reagents and solvents were obtained commercially and used without further purification. Thin layer chromatography (TLC) was performed on aluminium sheets precoated with silica gel 60 F_{254} (0.2 mm). Chromatographic spots were visualized using UV-detection and/or 2% ninhydrin in ethanol solution followed by heating. Column chromatography was performed using silica gel 60 (40–63 μM). Analytical HPLC–MS was performed on a Gilson-Finnigan ThermoQuest AQA system equipped with a C18 (Onyx Monolithic C18 (50 × 4.6 mm)) or a C4 (Hichrom ACE C4 (5 μm, 50 × 4.6 mm)) column using MeCN/H_2O (0.05% HCOOH) or MeOH/H_2O (0.05% HCOOH) with UV (254 nM) and MS (ESI) detection or on a Dionex UltiMate 3000 equipped with a C18 (Phenomenex Kinetex C18 (50 × 3.00 mm) column using MeCN/H_2O (0.05% HCOOH) UV (254) and MS (ESI IonTrap) detection or on a manual system equipped with a C8 (Zorbax SB-C8 (4.8 × 50 mm)) column using UV (220 nm) detection. Preparative HPLC was performed on a Gilson-Finigan ThermoQuest AQA system equipped with a C8 (Zorbax SB-C8 (5 μm, 150 × 21.2 mm)) column using MeCN/H_2O (0.05% HCOOH) as the mobile phase with UV (254 nm) detection or on a manual system equipped with a C8 (Zorbax SB-C8 (5 μm, 150 × 21.2 mm)) column using UV detection and MeCN/H_2O (0.05% HCOOH), MeCN/H_2O (0.1% TFA), or MeCN/H_2O with 25 mM NH_4OAc, pH 6,3 as the mobile phase. Purity determinations were done by RP-HPLC using the following conditions (UV detection at 254 nm): System 1 (ACE 5 C8 A3071, 50 × 4.6 mm, MeCN/H_2O with 0.1% TFA) and system 2 (Restec Allure Biphenyl, 50 × 4.6 mm, MeCN/H_2O with 0.1% TFA). Microwave reactions were carried out in a SmithSynthesizer™ or in an Initiator™ single-mode microwave cavity producing controlled irradiation at 2450 MHz. NMR spectra were recorded on a Varian Mercury plus spectrometer (^{1}H at 399.8 MHz, ^{13}C at 100.5 MHz) at ambient temperature. Chemical shifts (δ) are reported in ppm, indirectly referenced to tetramethylsilane (TMS) via the solvent signal (^{1}H: $CHCl_3$ δ 7.26, CD_2HOD δ 3.31; ^{13}C: $CDCl_3$ δ 77.16, CD_3OD δ 49.00). Exact molecular masses were determined on Micromass Q-Tof2 mass spectrometer equipped with an electrospray ion source.

7.1.1. Compound 1 (*tert*-butyl (2-((but-3-en-1-ylsulfonyl)carbamoyl)phenyl)carbamate)

Boc-Abz-OH (522 mg, 2.2 mmol) was dried in vacuo overnight over P_2O_5. Boc-Abz-OH and CDI (714 mg, 4.4 mmol) were dissolved in dry THF (40 mL) under N_2 atmosphere. The solution was stirred at 66 °C for 2 h before but-3-ene-1-sulfonamide (595 mg, 4.4 mmol), prepared as described earlier,[39] dissolved in dry THF (4 mL) was added together with DBU (991 μL, 6.6 mmol) under N_2 atmosphere. The reaction was then stirred for 2 h in r.t. THF was evaporated and DCM (40 mL) was added. The solution was washed with 5% citric acid and brine before the organic phase was evaporated. The product was purified on silica gel (CH_2Cl_2/MeOH 93:7) yielding **1** (464 mg, 59%) as a white solid. ^{1}H NMR ($CDCl_3$) δ: 8.44 (dd, J = 1.2, 8.6 Hz, 1H), 7.58–7.51 (m, 2H), 7.05 (ddd, J = 1.2, 7.2, 8.1 Hz, 1H), 5.82 (m,

1H), 5.21–5.10 (m, 2H), 3.70–3.65 (m, 2H), 2.69–2.62 (m, 2H), 1.52 (s, 9H). ^{13}C NMR ($CDCl_3$/CD_3OD 50:50) δ: 169.0, 153.2, 141.4, 134.7, 133.7, 129.1, 121.8, 120.1, 117.6, 117.1, 81.2, 52.7, 28.3, 27.5. MS calcd for $C_{16}H_{22}N_2O_5S$ $[M+H]^+$ 355.1, found: 355.1.

7.1.2. Compound 2 (*tert*-butyl(2-((pent-4-en-1-ylsulfonyl)carbamoyl)phenyl)carbamate)

Boc-Abz-OH (522 mg, 2.2 mmol) was dried in vacuo overnight over P_2O_5. Boc-Abz-OH and CDI (714 mg, 4.4 mmol) were dissolved in dry THF (40 mL) under N_2 atmosphere. The solution was stirred at 66 °C for 2.5 h before pent-4-ene-1-sulfonamide (657 mg, 4.4 mmol), prepared as described earlier,[39] dissolved in dry THF (4 mL) was added together with DBU (991 μL, 6.6 mmol) under N_2 atmosphere. The reaction was then stirred for 4 h. THF was evaporated and DCM (40 mL) was added. The solution was washed with 5% citric acid and brine before the organic phase was evaporated. The product was purified on silica gel (CH_2Cl_2/MeOH 93:7) followed by aluminium oxide (CH_2Cl_2/MeOH 93:7 then CH_2Cl_2/MeOH/HCOOH 95:5:1) yielding **2** (648 mg, 80%) as a white solid. ^{1}H NMR ($CDCl_3$) δ: 9.82 (s, 1H), 8.41 (dd, J = 1.2, 9.2 Hz, 1H), 7.56–7.51 (m, 2H), 5.80–5.69 (m, 2H), 5.11–5.04 (m, 2H), 3.60–3.55 (m, 2H), 2.27–2.20 (m, 2H), 2.04–1.95 (m, 2H), 1.52 (s, 9H). ^{13}C NMR ($CDCl_3$) δ: 167.7, 153.0, 142.1, 136.1, 135.2, 128.0, 121.8, 120.6, 117.0, 116.0, 81.2, 53.2, 31.9, 28.4, 22.5. MS calcd for $C_{17}H_{24}N_2O_5S$ $[M+H]^+$, 369.1, found: 369.2.

7.1.3. Compound 3 ((*S*)-*tert*-butyl (1-oxo-1-(pent-4-en-1-ylsulfonamido)pentan-2-yl)carbamate)

Prepared as described by us previously.[31]

7.1.4. 4-Chloro-6-methoxy-2-phenylpyrimidine

4,6-Dichloro-2-phenylpyrimidine (5.0 g, 22.2 mmol) and $NaOCH_3$ (3.6 g, 66.6 mmol) was stirred in methanol (500 mL) on an ice bath for 1 h, then brought to reflux for 7 h. After evaporation, the white solid was dissolved in DCM (100 mL) and washed with water. Evaporation of the organic phase yielded **8** (3.98 g, 81%) as a white solid. ^{1}H NMR (CD_3OD): δ 8.39–8.36 (m, 2H), 7.53–7.44 (m, 3H), 6.76 (s, 1H), 4.08 (s, 3H). ^{13}C NMR (CD_3OD): δ 172.3, 165.9, 162.2, 137.4, 132.6, 129.5, 129.5, 106.0, 55.0. MS calcd for $C_{11}H_9ClN_2O$ $[M+H]^+$ 221.0, found: 221.0.

7.1.5. Compound 4 ((*S*)-2-((*tert*-butoxycarbonyl)amino)-2-(4-hydroxyphenyl)acetic acid)

Prepared as described by us previously.[30]

7.1.6. Compound 5 ((*S*)-2-(3-bromo-4-hydroxyphenyl)-2-((*tert*-butoxycarbonyl)amino)acetic acid)

Prepared as described by us previously.[31]

7.1.7. Compound 6 ((*S*)-2-((*tert*-butoxycarbonyl)amino)-2-(4-((6-chloro-2-phenylpyrimidin-4-yl)oxy)phenyl)acetic acid)

Compound **4** (535 mg, 2.0 mmol), commercially available fenclorim (900 mg, 4.0 mmol) and KO*t*Bu (449 mg, 4.0 mmol) were dried overnight in vacuo over P_2O_5. Dry DMSO (8 mL) was added to the sealed reaction vial containing KO*t*Bu under N_2 atmosphere. Compound **4**, dissolved in DMSO (6 mL) was added to the reaction vial, and the reaction mixture was stirred for 30 min. Fenclorim, dissolved in DMSO (12 mL) was added to the reaction mixture and stirred at rt for 4 h. Water (150 mL) was added and pH adjusted to 11 with 2 M KOH. The mixture was washed with Et_2O before the aqueous phase was acidified using 1 M HCl to pH 2.75 so a precipitate was formed. Filtration of the precipitate yielded **6** (833 mg, 91%) as a white solid. ^{1}H NMR (CD_3OD): δ 8.20–8.16 (m, 2H), 7.55 (d, J = 8.7 Hz, 2H), 7.47 (m, 1H), 7.41–7.36 (m, 2H), 7.25 (d, J = 8.7 Hz, 2H), 6.94 (s, 1H), 5.27 (s, 1H), 1.47 (s, 9H). ^{13}C NMR (CD_3OD): δ 174.2, 171.9, 166.1, 163.4, 157.5, 153.6, 137.0, 136.8, 132.8, 130.0, 129.6, 129.5, 122.8, 106.4, 80.9, 58.9, 28.7. MS calcd for $C_{23}H_{22}ClN_3O_5$ $[M+H]^+$ 455.1, 457.1, found: 455.8, 457.8.

7.1.8. Compound 7 ((*S*)-2-((*tert*-butoxycarbonyl)amino)-2-(4-((2-phenyl-6-vinylpyrimidin-4-yl)oxy)phenyl)acetic acid)

Compound **6** (402 mg, 0.9 mmol), 2,4,6-trivinylcyclotriboroxane pyridine complex (432 mg, 1.8 mmol), $Pd(OAc)_2$ (21.6 mg, 0.09 mmol), $[(t\text{Bu})_3PH]BF_4$ (52.2 mg, 0.18 mmol), K_2CO_3 (744 mg, 5.4 mmol), H_2O (5.4 mL), and DME (18 mL) were mixed and divided into six 5 mL microwave process vials. The vials were sealed and exposed to microwave heating at 100 °C for 15 min. After filtration, the reaction mixtures were pooled and H_2O (55 mL) was added. 1 M NaOH was added until the pH was 10. The aqueous phase was washed with Et_2O and acidified with 2 M HCl to pH 2.85. Filtration of the formed precipitate yielded **7** (333 mg, 83%) as a white solid. ^{1}H NMR (CD_3OD): δ 8.27–8.24 (m, 2H), 7.53 (d, J = 8.5 Hz, 2H), 7.46–7.36 (m, 3H), 7.25 (d, J = 8.5 Hz, 2H), 6.87–6.79 (m, 2H), 6.61 (dd, J = 1.5, 17.3 Hz, 1H), 5.70 (dd, J = 1.5, 10.5 Hz, 1H), 5.27 (s, 1H), 1.47 (s, 9H). ^{13}C NMR (CD_3OD): δ 173.0, 170.8, 165.1, 164.2, 156.3, 152.8, 137.2, 135.1, 135.0, 130.8, 128.8, 128.2 (2 carbons), 122.0, 121.7, 102.6, 79.7, 57.6, 27.5. MS calcd for $C_{25}H_{25}N_3O_5$ $[M+H]^+$ 448.2, found: 447.9.

7.1.9. Compound 8 ((*S*)-2-((*tert*-butoxycarbonyl)amino)-2-(4-((6-methoxy-2-phenylpyrimidin-4-yl)oxy)phenyl)acetic acid)

Compound **4** (962 mg, 3.6 mmol), 4-chloro-6-methoxy-2-phenylpyrimidine (396 mg, 1.8 mmol) and KO*t*Bu (806 mg, 7.2 mmol) were dried overnight in vacuo over P_2O_5. The amounts of **4** and KO*t*Bu were divided into two reaction vials. Dry DMSO (H_2O <0.005%) (4 mL) was added to each reaction vial containing 4 and KO*t*Bu. The vials were sealed under nitrogen and the reaction mixture stirred for 40 min before 4-chloro-6-methoxy-2-phenylpyrimidine dissolved in DMSO (5 mL) was added to each vial. The reactions were heated at 64 °C overnight. The reactions were pooled, filtered and diluted with water (150 mL) before extraction with ethyl acetate. After evaporation of the organic phase and purification on silica gel (CH_2Cl_2/MeOH 90:10, then CH_2Cl_2/MeOH/AcOH 95:5:3) **8** (596 mg, 70%) was obtained as a white solid. ^{1}H NMR (CD_3OD): δ 8.26–8.24 (m, 2H), 7.52 (d, J = 8.8 Hz, 2H), 7.45 (m, 1H), 7.42–7.37 (m, 2H), 7.21–7.18 (m, 2H), 6.06 (s, 1H), 4.86 (s, 1H), 4.06 (s, 3H), 1.46 (s, 9H). ^{13}C NMR (CD_3OD): δ 174.1, 173.7, 172.6, 165.2, 157.5, 154.3, 138.1, 136.0, 132.1, 130.0, 129.3 (2 carbons), 122.8, 90.0, 81.0, 58.7, 54.7, 28.7. MS calcd for $C_{24}H_{25}N_3O_6$ $[M+H]^+$ 452.1, found: 452.1.

7.1.10. Compound 9 ((*S*)-2-(3-bromo-4-((6-methoxy-2-phenylpyrimidin-4-yl)oxy)phenyl)-2-((*tert*-butoxycarbonyl)amino)acetic acid)

Compound **5** (2.0 g, 5.7 mmol), 4-chloro-6-methoxy-2-phenylpyrimidine (1.9 g, 8.6 mmol) and KO*t*Bu (1.5 g, 2.2 mmol) were dried overnight in vacuo over P_2O_5. Dry DMSO (H_2O <0.005%) (40 mL) was added to a vial containing **5** and KO*t*Bu. The vial was sealed under nitrogen and stirred for 40 min before 4-chloro-6-methoxy-2-phenylpyrimidine dissolved in DMSO (40 mL) was added. The reaction was heated at 64 °C for 2 days. The reaction mixture was filtered, diluted with water (500 mL), and extracted with petroleum ether. The aqueous phase was acidified with 1 M HCl to pH 3. Filtration of the precipitate yielded **9** (2.6 g, 87%) as a white solid. ^{1}H NMR (CD_3OD) δ 8.17 (m, 2H), 7.78 (d, J = 2.2 Hz, 1H), 7.51 (dd, J = 2.1, 8.3 Hz, 1H), 7.42 (m, 1H), 7.38–7.33 (m, 2H), 7.29 (d, J = 8.4 Hz, 1H), 6.14 (s, 1H), 5.28 (s, 1H), 4.07 (s, 3H), 1.47 (s, 9H). ^{13}C NMR ($CDCl_3$) δ: 172.8, 172.3, 170.4, 163.9, 156.9, 150.1, 137.3, 136.9, 132.4, 131.1, 128.5, 128.4, 127.3, 124.1, 116.7, 89.1, 82.4, 58.1, 54.3, 28.3. MS calcd for $C_{24}H_{24}BrN_3O_6$ $[M+H]^+$: 530.1, 532.1, found: 530.1, 532.1.

7.1.11. Compound 10 ((*S*)-2-((*tert*-butoxycarbonyl)amino)-2-(4-((6-methoxy-2-phenylpyrimidin-4-yl)oxy)-3-vinylphenyl)acetic acid)

Compound **9** (705.3 mg, 1.33 mmol), 2,4,6-trivinylcycloboroxane pyridine complex (591.5 mg, 2.66 mmol), $Pd(OAc)_2$ (32.2 mg, 0.133 mmol), $[(t\text{Bu})_3\text{PH}]BF_4$ (77 mg, 0.266 mmol), K_2CO_3 (1.11 g, 8.1 mmol), DME (26.6 mL) and water (8 mL) were mixed in seven 5 mL microwave vials. The vials were sealed and exposed to microwave heating at 100 °C for 15 min. After centrifugal filtration, and pooling of the reaction mixtures, the DME was evaporated. Water (35 mL) was added and the reaction mixture was acidified with 5% HCl to pH 1. Filtration of the precipitate yielded **10** (518 mg, 82%) as a white solid. ^{1}H NMR (CD_3OD) δ: 8.26–8.22 (m, 2H), 7.78 (d, J = 2.3 Hz, 1H), 7.47–7.36 (m, 4H), 7.15 (d, J = 8.3 Hz, 1H), 6.79 (dd, J = 11.4, 17.4 Hz, 1H), 6.00 (s, 1H), 5.86 (dd, J = 1.3, 17.8 Hz, 1H), 5.28 (dd, J = 1.3, 11.4 Hz, 1H), 5.20 (s, 1H), 4.06 (s, 3H), 1.46 (s, 9H). ^{13}C NMR (CD_3OD) δ: 174.6, 173.8, 172.7, 165.3, 157.5, 151.0, 138.1, 137.5, 132.1, 132.0, 131.5, 129.3 (2 carbons), 129.1, 126.9, 123.8, 117.1, 89.5, 80.8, 59.3, 54.7, 28.7. MS calcd for $C_{26}H_{27}N_3O_6$ $[M+H]^+$ 478.2, found: 478.2.

7.1.12. General procedure A, for N-deprotection (compounds 1–3, 13–15, 23–25, and 37)

The respective carbamate was dissolved in 4.0 M HCl in 1,4-dioxane (10 mL/mmol starting material) and stirred at room temperature until starting material could no longer be visualized by LC–MS. The solvent was thereafter evaporated and the hydrochloride salt of the N-deprotected product was used in forthcoming couplings without further purification.

7.1.13. Compound 11 (*tert*-butyl ((*S*)-2-oxo-2-(((*S*)-1-oxo-1-(pent-4-en-1-ylsulfonamido)pentan-2-yl)amino)-1-(4-((2-phenyl-6-vinylpyrimidin-4-yl)oxy)phenyl)ethyl)carbamate)

Compound **7** (64 mg, 0.143 mmol) was mixed with the N-deprotected HCl-salt of **3** (26.4 mg, 0.172 mmol), HATU (65 mg, 0.172 mmol) and DIEA (142 μL, 0.829) and stirred in DMF for 2 h. Addition of ethyl acetate (20 mL) before work up and purification on silica gel (CH_2Cl_2/MeOH 95:5) yielded **11** (74.2 mg, 77%) as a white solid. ^{1}H NMR ($CDCl_3$): δ 10.12 (s, 1H), 8.35–8.30 (m, 2H), 7.47–7.38 (m, 5H), 7.24 (d, J = 8.7 Hz, 2H), 6.96 (d, J = 7.7 Hz, 1H), 6.75 (dd, J = 10.4, 17.2 Hz, 1H), 6.62 (s, 1H), 6.60 (dd, J = 1.7, 17.2 Hz, 1H), 5.78–5.62 (m, 3H), 5.26 (s, 1H), 5.04–4.96 (m, 2H), 4.58 (m, 1H), 3.41–3.26 (m, 2H), 2.15–2.08 (m, 2H), 1.92–1.81 (m, 3H), 1.71 (m, 1H), 1.46 (s, 9H), 1.42–1.33 (m, 2H), 0.91 (t, J = 7.3 Hz, 3H). ^{13}C NMR ($CDCl_3$): δ 171.2, 170.2, 164.9, 164.4, 162.9, 155.9, 153.1, 137.2, 136.4, 135.2, 133.7, 131.0, 128.7, 128.5 (2 carbons), 122.9, 122.4, 116.6, 102.7, 81.4, 59.0, 54.1, 52.7, 33.7, 31.9, 28.4, 22.2, 18.8, 13.7. MS calcd for $C_{37}H_{45}N_5O_7S$ $[M+H]^+$ 678.3, found: 677.9.

7.1.14. General procedure B, for synthesis of compounds 12–15 and 37

The N-deprotected HCl-salts of P1–P1′ building blocks **1** or **2** were mixed with P2 building blocks **7**, **8**, **10** or **36** and HATU in dry DCM. DIEA was added until the pH exceeded 10. The reactions were stirred at 45 °C. When starting material no longer could be visualized by LC–MS, DCM was added and the reaction mixture was washed with 0.1 M $NaHSO_4$ followed by 0.035 M $NaHSO_4$. The organic phase was thereafter evaporated before purification.

7.1.15. Compound 12 ((*S*)-*tert*-butyl(2-oxo-2-((2-((pent-4-en-1-ylsulfonyl)carbamoyl)phenyl)amino)-1-(4-((2-phenyl-6-vinylpyrimidin-4-yl)oxy)phenyl)ethyl)carbamate)

Prepared according to the general procedure B described above, using **7** (44.7 mg, 0.10 mmol), the N-deprotected HCl-salt of **2** (36.6 mg, 0.12 mmol), HATU (45.6 mg, 0.12 mmol), and DIEA (99 μL, 0.58 mmol). The reaction was stirred in dry DCM (5 mL) at 45 °C for 2 h. Addition of DCM before workup and purification on silica gel (CH_2Cl_2/MeOH 93:7), gave **12** (67 mg, 96%) as a white solid. ^{1}H NMR (CD_3OD):δ 8.48 (m, 1H), 8.22–8.18 (m, 2H), 8.11 (m, 1H), 7.70 (d, J = 8.6 Hz, 2H), 7.44–7.35 (m, 2H), 7.31–7.21 (m, 4H), 7.08 (ddd, J = 1.2, 7.3, 8.0 Hz, 1H), 6.82 (s, 1H), 6.81 (dd, J = 10.5, 17.3 Hz, 1H), 5.75–5.63 (m, 2H), 5.34 (s, 1H), 4.98–4.85 (m, 2H), 3.31–3.24 (m, 2H), 2.12–2.04 (m, 2H), 1.91–1.82 (m, 2H), 1.48 (s, 9H). ^{13}C NMR (CD_3OD): δ 173.8, 172.0, 171.3, 166.3, 165.3, 157.5, 154.1, 140.7, 138.5, 138.3, 136.3, 136.1, 133.2, 133.9, (2 carbons), 130.3, 129.4, 129.3, 125.0, 124.0, 123.2, 123.1, 121.2, 116.1, 103.7, 81.1, 61.8, 53.0, 33.5, 28.8, 24.3. MS calcd for $C_{37}H_{39}N_5O_7S$ $[M+H]^+$ 698.3, found: 698.3. HPLC purity (system 1: 96.2%, system 2: 97.9%).

7.1.16. Compound 13 ((*S*)-*tert*-butyl(1-(4-((6-methoxy-2-phenylpyrimidin-4-yl)oxy)phenyl)-2-oxo-2-((2-((pent-4-en-1-ylsulfonyl)carbamoyl)phenyl)amino)ethyl)carbamate)

Prepared according to the general procedure B, using the N-deprotected HCl-salt of **2** (99.3 mg, 0.33 mmol), **8** (144 mg, 0.27 mmol), HATU (124 mg, 0.33 mmol), and DIEA (269 μL, 1.57 mmol). The reaction was stirred in DCM for 3 h. Purification on silica gel (CH_2Cl_2/MeOH 90:10) yielded **13** (162 mg, 86%) as a white solid. ^{1}H NMR (CD_3OD): δ 8.49 (m, 1H), 8.20–8.17 (m, 2H), 8.15 (m, 1H), 7.69–7.66 (m, 2H), 7.43–7.35 (m, 2H), 7.31–7.26 (m, 2H), 7.17 (d, J = 8.6 Hz, 2H), 7.04 (m, 1H), 6.06 (s, 1H), 5.67 (m, 1H), 5.33 (s, 1H), 4.96–4.84 (m, 2H), 4.03 (s, 3H), 3.26–3.18 (m, 2H), 2.11–2.02 (m, 2H), 1.92–1.83 (m, 2H), 1.46 (s, 9H). ^{13}C NMR (CD_3OD): δ 174.2, 173.7, 172.5, 171.2, 165.1, 157.4, 154.4, 140.8, 138.5, 138.0, 136.0, 133.3, 132.2, 132.0, 130.3, 129.3 (2 carbons), 124.8, 123.9, 123.0, 121.1, 116.1, 90.0, 81.1, 61.8, 54.7, 53.2, 33.4, 28.7, 24.2. HRMS calcd for $C_{36}H_{39}N_5O_8S$ $[M+H]^+$ 702.2598, found: 702.2601. HPLC purity (system 1: 98.6%, system 2: 99.6%).

7.1.17. Compound 14 ((*S*)-*tert*-butyl(1-(4-((6-methoxy-2-phenylpyrimidin-4-yl)oxy)-3-vinylphenyl)-2-oxo-2-((2-((pent-4-en-1-ylsulfonyl)carbamoyl)phenyl)amino)ethyl)carbamate)

Prepared according to the general procedure B, using **10** (119 mg, 0.25 mmol), the N-deprotected HCl-salt of **1** (110 mg, 0.38 mmol), HATU (114 mg, 0.3 mmol), and DIEA (273 μL, 1.6 mmol). The reaction was stirred in DCM for 2 h. Purification on silica gel (CH_2Cl_2/MeOH 94:6) followed by purification on preparative HPLC (MeCN/H_2O (0.05% HCOOH)) yielded **14** (13.1 mg, 7%) as a white solid. ^{1}H NMR (CD_3OD): δ 8.24 (dd, J = 1.2, 8.4 Hz, 1H), 8.20 (dd, J = 1.4, 8.5 Hz, 2H), 7.86 (d, J = 2.4 Hz, 1H), 7.75 (dd, J = 1.6, 7.9 Hz, 1H), 7.59 (dt, J = 1.6, 7.5 Hz, 1H), 7.48 (dd, J = 2.4, 8.5 Hz, 1H), 7.41 (m, 1H), 7.34–7.30 (m, 2H), 7.25 (ddd, J = 1.1, 7.4, 7.9 Hz, 1H), 7.20 (d, J = 8.3 Hz, 1H), 6.81 (dd, J = 11.3, 17.8 Hz, 1H), 6.05 (s, 1H), 5.94 (d, J = 17.8 Hz, 1H), 5.76 (m, 1H), 5.40 (s, 1H), 5.31 (d, J = 11.2 Hz, 1H), 5.09 (d, J = 17.2 Hz, 1H), 4.98 (d, J = 10.2 Hz, 1H), 4.05 (s, 3H), 3.55–3.50 (m, 2H), 2.58–2.51 (m, 2H), 1.49 (s, 9H). ^{13}C NMR (CD_3OD): δ 173.7, 173.5, 172.6, 171.3, 165.2, 157.5, 151.3, 140.7, 138.0, 136.7, 136.6, 133.2, 132.3, 132.0, 131.8, 131.3, 129.4, 129.3, 127.3, 124.9, 124.2, 124.0, 121.2, 117.7, 116.5, 89.0, 81.1, 61.9, 54.7, 52.6, 29.1, 28.7. HRMS calcd for $C_{37}H_{39}N_5O_8S$ $[M+H]^+$ 714.2598, found: 714.2606. HPLC purity (system 1: 100%, system 2: 100%).

7.1.18. Compound 15 ((*S*)-*tert*-butyl(1-(4-((6-methoxy-2-phenylpyrimidin-4-yl)oxy)-3-vinylphenyl)-2-oxo-2-((2-((pent-4-en-1-ylsulfonyl)carbamoyl)phenyl)amino)ethyl)carbamate)

Prepared according to the general procedure B using the N-deprotected HCl-salt of **2** (40.5 mg, 0.13 mmol), **10** (40 mg, 0.083 mmol), HATU (38 mg, 0.10 mmol) and DIEA (92 μL, 0.53 mmol). The reaction was stirred in DCM overnight. Purification on preparative HPLC (MeCN/H_2O (0.05% HCOOH)) yielded **15** (10.8 mg, 18%) as a white solid. ^{1}H NMR (CD_3OD): δ 8.24 (d, J = 8.4 Hz, 1H), 8.20 (dd, J = 1.5, 8.3 Hz, 2H), 7.86 (d, J = 2.4 Hz, 1H), 7.75 (dd, J = 1.5, 8.0 Hz, 1H), 7.60 (m, 1H), 7.48 (dd, J = 2.4,

8.4 Hz, 1H), 7.41 (dt, *J* = 1.2, 7.5 Hz, 1H), 7.33–7.29 (m, 2H), 7.25 (ddd, *J* = 1.2, 8.0 Hz, 1H), 7.20 (d, *J* = 8.4, 1H), 6.81 (dd, *J* = 11.1, 17.6 Hz, 1H), 6.06 (s, 1H), 5.94 (dd, *J* = 1.2, 17.6 Hz, 1H), 5.75 (m, 1H), 5.40 (s, 1H), 5.31 (dd, *J* = 1.2, 11.1 Hz, 1H), 5.05–4.95 (m, 2H), 4.06 (s, 3H), 3.44 (m, 2H), 2.15 (m, 2H), 1.88 (m, 2H), 1.49 (s, 9H). ^{13}C NMR (CD_3OD): δ 173.8, 172.6, 171.2, 169.9, 165.3, 157.7, 151.4, 139.7, 138.1, 136.6, 134.9, 132.4, 132.1, 131.4, 130.3, 129.4, 129.3 (2 carbons), 127.6, 125.2, 124.3, 123.2, 122.4, 117.6, 116.5, 89.7, 81.3, 61.1, 54.8, 53.5, 33.0, 28.7, 23.6. HRMS calcd for $C_{38}H_{41}N_5O_8S$ $[M+H]^+$ 728.2676, found 728.2150. HPLC purity (system 1: 98.8%, system 2: 98.7%).

7.1.19. Compound 16 (but-3-en-1-yl((*S*)-3,3-dimethyl-1-oxo-1-(((*S*)-2-oxo-2-((2-((pent-4-en-1-ylsulfonyl)carbamoyl)phenyl)amino)-1-(4-((2-phenyl-6-vinylpyrimidin-4-yl)oxy)phenyl)ethyl)amino)butan-2-yl)carbamate)

Compound **12** (56.7 mg, 0.081 mmol) was stirred in CH_2Cl_2/TFA 1:1 (2 mL) for 1 h. After evaporation of the solvent the N-deprotected TFA-salt of **12** was mixed with *N*-[(But-3-en-1-yloxy)carbonyl]-3-methyl-L-valine[44] (26 mg, 0.11 mmol), HATU (52 mg, 0.14 mmol), and DIEA (96 μL). The reaction was stirred in dry DMF at room temperature for 1 h. Ethyl acetate (15 mL) was added and the reaction mixture was washed with 0.1 M $NaHSO_4$ followed by 0.035 M $NaHSO_4$ before evaporation of the organic phase. Purification by preparative HPLC (MeCN/H_2O (0.1% TFA)) yielded **16** (2.9 mg, 4%) as a white solid. ^{1}H NMR (CD_3OD): δ 8.25–8.22 (m, 2H), 8.15 (m, 1H), 7.71 (dd, *J* = 1.4, 7.8 Hz, 1H), 7.67–7.65 (m, 2H), 7.59 (ddd, *J* = 1.5, 7.4, 8.3 Hz, 1H), 7.41 (m, 1H), 7.36–7.30 (m, 4H), 7.25 (ddd, *J* = 1.2, 7.5, 7.9 Hz, 1H), 6.88 (s, 1H), 6.84 (dd, *J* = 10.7, 17.3 Hz, 1H), 5.86–5.69 (m, 3H), 5.66 (s, 1H), 5.12–4.93 (m, 4H), 4.13 (s, 1H), 4.11–4.04 (m, 2H), 3.46–3.40 (m, 2H), 2.40–2.33 (m, 2H), 2.17–2.10 (m, 2H), 1.91–1.82 (m, 2H), 1.06 (s, 9H). ^{13}C NMR (CD_3OD): δ173.1, 171.9, 170.2, 169.9, 166.3, 165.7, 165.4, 154.4, 139.5, 138.4, 138.1, 136.3, 135.5, 135.2, 134.7, 132.0, 130.7, 130.3, 129.4 (2 carbons), 125.3, 123.6, 123.3, 117.5, 116.5, 103.9, 65.5, 64.2, 59.7, 53.5, 35.5, 34.7, 33.0, 27.3, 23.6. HRMS calcd for $C_{43}H_{48}N_6O_8S$ $[M+H]^+$ 809.3333, found: 809.3340. HPLC purity (system 1: 98.8%, system 2: 98.2%).

7.1.20. Compound 17 (*tert*-butyl((*S*)-1-(((*S*)-1-(4-((6-methoxy-2-phenylpyrimidin-4-yl)oxy)phenyl)-2-oxo-2-((2-((pent-4-en-1-ylsulfonyl)carbamoyl)phenyl)amino)ethyl)amino)-1-oxonon-8-en-2-yl)carbamate)

The N-deprotected HCl-salt of **13** (73 mg, 0.11 mmol) was mixed with Boc-2-amino-8-nonenoic acid (46 mg, 0.17 mmol), HATU (78 mg, 0.21 mmol), and 4-methylmorpholine (116 μL, 0.88 mmol). The reaction was stirred in DMF (2 mL) at room temperature for 2 h. Ethyl acetate (15 mL) was added and the reaction mixture was washed with 0.1 M $NaHSO_4$ followed by 0.035 M $NaHSO_4$, whereafter the organic phase was evaporated. Purification on silica gel (CH_2Cl_2/MeOH 93:7) yielded **17** (76.4 mg, 79%. A small fraction was purified on HPLC (MeCN/H_2O (0.05% HCOOH)). ^{1}H NMR (CD_3OD, purified on silica gel): δ 8.45(dd, *J* = 1.3, 8.1 Hz, 1H), 8.23–8.19 (m, 2H), 8.15 (dd, *J* = 1.7, 8.0 Hz, 1H), 7.71 (d, *J* = 8.7 Hz, 2H), 7.42–7.37 (m, 2H), 7.35–7.29 (m, 2H), 7.22–7.19 (m, 2H), 7.07 (m, 1H), 6.08 (s, 1H), 5.85–5.61 (m, 3H), 4.97–4.86 (m, 4H), 4.21 (m, 1H), 4.05 (s, 3H), 3.78 (s, 1H), 3.28–3.16 (m, 2H), 2.11–2.01 (m, 3H), 1.99–1.92 (m, 2H), 1.88–1.79 (m, 3H), 1.74–1.64 (m, 2H), 1.42 (s, 9H), 1.33–1.25 (m, 2H). ^{13}C NMR (CD_3OD, purified on silica gel): δ 175.3, 173.8, 173.7, 172.5, 170.3, 165.1, 157.9, 154.5, 140.6, 140.0, 138.6, 138.0, 135.6, 133.0, 132.0, 131.8, 130.3, 129.4, 129.3, 125.2, 124.1, 123.1, 121.3, 116.0, 114.7, 90.0, 80.7, 60.4, 56.5, 54.7, 52.9, 34.7, 33.5, 33.2, 29.9, 28.7, 26.8, 24.3. ^{1}H NMR (CD_3OD, purified on HPLC): δ 8.26–8.22 (m, 2H), 8.17 (m, 1H), 7.73 (dd, *J* = 1.8, 8.2 Hz, 1H), 7.63 (d, *J* = 8.6 Hz, 2H), 7.58 (m, 1H), 7.43 (m, 1H), 7.73 (dd, *J* = 1.8, 8.2 Hz, 1H), 7.63 (d, *J* = 8.6 Hz, 2H), 7.58 (m, 1H), 7.43 (m, 1H), 7.39–7.33 (m, 2H), 7.29–7.24 (m, 2H), 7.23 (d, *J* = 1.2 Hz, 1H), 6.11 (s, 1H), 5.83–5.69 (m, 2H), 5.64 (s, 1H), 5.04–4.87 (m, 4H), 4.17 (m, 1H), 4.07 (s, 3H), 3.49–3.40 (m, 2H), 2.19–2.11 (m, 3H), 2.04–1.97 (m, 2H), 1.92–1.83 (m, 3H), 1.71–1.61 (m, 2H), 1.42 (s, 9H), 1.38–1.30 (m, 2H). ^{13}C NMR (CD_3OD, purified on HPLC): δ 175.3, 173.8, 172.6, 170.4, 170.0, 165.3, 158.1, 154.6, 140.0, 139.4, 138.1(2 carbon), 135.5, 134.7, 132.1, 130.8, 130.6, 130.3, 129.4 (2 carbons), 125.3, 123.5, 123.1, 116.5, 114.8, 90.1, 80.7, 59.6, 56.1, 54.7, 53.5, 34.8, 33.0, 30.0 (2 carbons), 28.7, 26.7, 23.6. HRMS calcd for $C_{45}H_{54}N_6O_9S$ $[M+H]^+$ 855.3751, found: 855.3748. HPLC purity (system 1: 96.9%, system 2: 97.8%).

7.1.21. General procedure C, for synthesis of compounds 18–19, 26–28, and 38

The N-deprotected HCl-salts of the P2–P1–P1′ building blocks were mixed with HATU and Boc-L-*t*Leu, or Boc-2-amino-8 nonenoic acid in dry DMF. DIEA was added until the pH exceeded 10. The reactions were stirred in room temperature until starting material could no longer be detected by LC–MS. Ethyl acetate was added and the reaction mixture washed with sodium acetate buffer pH 4. The organic phase was evaporated before purification on preparative HPLC.

7.1.22. Compound 18 (*tert*-butyl ((*S*)-1-(((*S*)-1-(4-((6-methoxy-2-phenylpyrimidin-4-yl)oxy)phenyl)-2-oxo-2-((2-((pent-4-en-1-ylsulfonyl)carbamoyl)phenyl)amino)ethyl)amino)-3,3-dimethyl-1-oxobutan-2-yl)carbamate)

Prepared according to the general procedure C, using the N-deprotected HCl-salt of **13** (17.0 mg, 0.027 mmol), Boc-L-*t*Leu (18.7 mg, 0.081 mmol), HATU (36.9 mg, 0.097 mmol), and DIEA (38.5 μL, 0.22 mmol). The reaction was stirred in DMF for 1.5 h. Purification on preparative HPLC (MeCN/H_2O with 25 mM NH_4OAc, pH 6.3) yielded **18** (7.9 mg, 35%), as the NH_4^+-salt, in a 5:2 L:D diastereomeric mixture. ^{1}H NMR ($CDCl_3$, major isomer reported): δ 8.55 (m, 1H), 8.32–8.25 (m, 3H), 7.61–7.52 (m, 3H), 7.42 (m, 1H), 7.37–7.31 (m, 2H), 7.23–7.20 (m, 2H), 7.13 (m, 1H), 5.98 (s, 1H), 5.72 (m, 1H), 5.24 (s, 1H), 5.08–5.00 (m, 2H), 4.06 (s, 3H), 3.99 (m, 1H), 3.56–3.40 (m, 2H), 2.22–2.15 (m, 2H), 1.99–1.90 (m, 2H), 1.40 (s, 9H), 1.05 (s, 9H). ^{13}C NMR ($CDCl_3$): δ 172.2, 171.2, 170.9, 168.6, 168.3, 164.2, 156.0, 153.4, 150.9, 140.3, 137.0, 136.4, 134.8, 134.1, 131.2, 129.1, 128.5 (2 carbons), 123.9, 122.3, 121.9, 118.5, 116.8, 89.2, 80.2, 62.7, 58.4, 54.2, 53.2, 34.7, 32.0, 28.5, 26.9, 22.5. HRMS calcd for $C_{42}H_{50}N_6O_9S$ $[M+H]^+$ 815.3438, found: 815.3436. HPLC purity (system 1: 98.2%, system 2: 99.7%).

7.1.23. Compound 19L (*tert*-butyl((*S*)-1-(((*S*)-1-(4-((6-methoxy-2-phenylpyrimidin-4-yl)oxy)-3-vinylphenyl)-2-oxo-2-((2-((pent-4-en-1-ylsulfonyl)carbamoyl)phenyl)am ino)ethyl) amino)-3,3-dimethyl-1-oxobutan-2-yl)carbamate) and 19D (*tert*-butyl((*S*)-1-(((*R*)-1-(4-((6-methoxy-2-phenylpyrimidin-4-yl)oxy)-3-vinylphenyl)-2-oxo-2-((2-((pent-4-en-1-ylsulfonyl)carbamoyl)phenyl)amino)ethyl)amino)-3,3-dimethyl-1-oxobutan-2-yl)carbamate)

Prepared following the general procedure C, using the N-deprotected HCl-salt of **15** (41.8 mg, 0.063 mmol), Boc-L-*t*Leu (23.3 mg, 0.10 mmol), HATU (28.7 mg, 0.075 mmol) and DIEA (94 μL, 0.54 mmol). The reaction was stirred in DMF for 5 h. Purification and separation of the diastereomers on preparative HPLC (MeCN/H_2O (0.05% HCOOH)) gave **19L** (8.1 mg, 15%) and **19D** (5.5 mg, 10%) as white solids. **19L** ^{1}H NMR (CD_3OD): δ 8.77 (d, *J* = 6.6 Hz, 1H), 8.20 (dd, *J* = 1.2, 8.3 Hz, 2H), 8.14 (dd, *J* = 1.2, 8.5, 1H), 7.92 (d, *J* = 2.4 Hz, 1H), 7.72 (dd, *J* = 1.6, 8.0 Hz, 1H), 7.59 (ddd, *J* = 1.5, 7.3, 8.2 Hz, 1H), 7.37 (dd, = 2.7, 8.4 Hz, 1H), 7.41 (m, 1H), 7.31 (t, *J* = 7.7 Hz, 2H), 7.25 (dt, *J* = 1.5, 7.8 Hz, 1H), 7.21 (d, *J* = 8.4 Hz, 1H), 6.82 (dd, *J* = 11.2, 17.9 Hz, 1H), 6.07 (s, 1H), 5.99 (d,

J = 17.6 Hz, 1H), 5.77–5.66 (m, 2H), 5.32 (dd, J = 1.2, 11.3 Hz, 1H), 5.02–4.93 (m, 2H), 4.06 (s, 3H), 3.44–3.32 (m, 2H), 2.12–2.05 (m, 2H), 1.88–1.79 (m, 2H), 1.42 (s, 9H), 1.05 (s, 9H). ^{13}C NMR (CD_3OD): δ 173.8, 173.4, 173.3, 172.6, 170.0, 169.8, 165.3, 158.0, 155.1, 151.5, 139.4, 138.1, 138.0, 135.9, 134.7, 132.5, 132.4, 132.1, 131.4, 130.2, 129.4, 129.3, 127.8, 125.3, 124.4, 123.6, 117.8, 116.5, 89.7, 80.8, 63.9, 59.6, 54.8, 35.3, 32.9, 28.7, 27.3, 23.5. HPLC purity (system 1: 100%, system 2 100%) **19D** ^{1}H NMR (CD_3OD): δ 8.84 (d, J = 6.9 Hz, 1H), 8.19 (dd, J = 2.0, 8.2 Hz, 2H), 8.05 (m, 1H), 7.91 (d, J = 2.3 Hz, 1H), 7.71 (dd, J = 1.5, 7.8 Hz, 1H), 7.59 (m, 1H), 7.52 (dd, J = 2.4, 8.2 Hz, 1H), 7.42 (tt, J = 1.5, 7.3 Hz, 1H), 7.32 (t, J = 7.6 Hz, 2H), 7.27 (dt, J = 1.2, 7.6 Hz, 1H), 7.22 (d, J = 8.2 Hz, 1H), 6.82 (dd, J = 11.3, 17.9 Hz, 1H), 6.08 (s, 1H), 5.98 (d, J = 17.8 Hz, 1H), 5.70 (dt, J = 6.7, 17.0 Hz, 2H), 5.32 (dd, J = 1.2, 11,3 Hz, 1H), 5.02–4.92 (m, 2H), 4.07(s, 3H), 3.40–3.30 (m, 2H) 2.06 (q, J = 7.1 Hz, 2H), 1.88–1.79 (m, 2H), 1.43 (s, 9H), 1.00 (s, 9H). ^{13}C NMR (CD_3OD): δ 179.1, 177.4, 173.8, 172.6, 169.7, 168.7, 165.3, 157.9, 151.5, 138.2, 138.1, 136.1, 134.4, 132.5, 132.1, 131.3, 130.1, 130.0, 129.4, 129.3, 127.9, 125.6, 124.4, 117.8, 116.4, 96.5, 89.7, 80.7, 64.1, 59.4, 54.8, 53.4, 35.4, 32.9, 28.8, 27.2, 23.6. HRMS calcd for $C_{44}H_{52}N_6O_9S$ $[M+H]^+$ 841.3594, found: 841.3596. HPLC purity (system 1: 100%, system 2 100%).

7.1.24. Compound 20 ((*S*)-methyl 2-((*tert*-butoxycarbonyl) amino)-2-(4-((2-phenyl-6-vinylpyrimidin-4-yl)oxy)phenyl) acetate)

7 (191 mg, 0.43 mmol) was mixed with Cs_2CO_3 (278 mg, 0.85 mmol) in a round bottomed flask. The flask was sealed under nitrogen. DMF (12 mL) was added and the reaction mixture was stirred for 30 min before MeI (53.4 μL, 0.85 mmol) was added. The reaction was then stirred at room temperature overnight. The reaction mixture was filtered before ethyl acetate (25 mL) was added. The reaction mixture was washed with saturated $NaHCO_3$ before the organic phase was evaporated. Purification on silica gel (EtOAc/*i*-hexane 25:75) yielded **20** (110.5 mg, 56%) as a white solid. ^{1}H NMR ($CDCl_3$): δ 8.36–8.32 (m, 2H), 7.47–7.38 (m, 5H), 7.26–7.23 (m, 2H), 6.77 (dd, J = 10.4, 17.1 Hz, 1H), 6.65 (s, 1H), 6.61 (dd, J = 1.5, 17.1 Hz, 1H), 5.70 (dd, J = 1.5, 10.5 Hz, 1H), 5.62 (s, 1H), 5.39 (s, 1H), 3.77 (s, 3H), 1.46 (s, 9H). ^{13}C NMR ($CDCl_3$): δ 171.8, 170.5, 164.9, 164.5, 155.1, 152.9, 137.4, 135.3, 134.2, 131.1, 128.6 (3 carbons), 122.9, 122.2, 102.8, 80.6, 57.3, 53.0, 28.5. MS calcd for $C_{26}H_{27}N_3O_5$ $[M+H]^+$ 462.2, found: 461.9.

7.1.25. Compound 21 (*S*)-methyl 2-((*S*)-2-(((but-3-en-1-yloxy) carbonyl)amino)-3,3-dimethylbutanamido)-2-(4-((2-phenyl-6-vinylpyrimidin-4-yl)oxy)phenyl)acetate

Compound **20** (65 mg, 0.14 mmol) was stirred in CH_2Cl_2/TFA 1:1 (4 mL) for 1 h. After evaporation of the solvent the N-deprotected TFA-salt of 20 was mixed with *N*-[(But-3-en-1-yloxy)carbonyl]-3-methyl-L-valine[44] (36 mg, 0.16 mmol), HATU (71 mg, 0.19 mmol), and DIEA (113 μL, 1.25 mmol). The reaction was stirred in dry DMF (1 mL) at room temperature for 1 h. Ethyl acetate (20 mL) was added and the reaction mixture was washed with 0.1 M $NaHSO_4$ followed by 0.035 M $NaHSO_4$ before evaporation of the organic phase. Purification on silica gel (CH_2Cl_2/MeOH 98:2) yielded **21** (50 mg, 62%). ^{1}H NMR ($CDCl_3$): δ 8.35–8.31 (m, 2H), 7.44–7.40 (m, 5H), 7.26–7.23 (m, 2H), 6.76 (dd, J = 10.4, 17.2 Hz, 1H), 6.64 (s, 1H), 6.61 (dd, J = 1.7, 17.2 Hz, 1H), 5.74 (m, 1H), 5.69 (dd, J = 1.7, 10.4 Hz, 1H), 5.58 (d, J = 6.7 Hz, 1H), 5.41 (d, J = 9.4 Hz), 5.10–5.01 (m, 2H), 4.13–4.00 (m, 3H), 3.77 (s, 3H), 2.36–2.30 (m, 2H), 1.05 (s, 9H). ^{13}C NMR ($CDCl_3$): δ 171.0, 170.4, 170.3, 164.8, 164.4, 156.7, 153.0, 137.2, 135.2, 134.2, 133.0, 131.1, 128.8, 128.5 (2 carbons), 123.0, 122.3, 117.3, 102.7, 64.4, 62.7, 56.2, 53.1, 35.0, 33.5, 26.7. MS calcd for $C_{32}H_{36}N_4O_6$ $[M+H]^+$ 573.3, found 573.0.

7.1.26. Compound 22L and 22D

In a microwave process vial, compound **21** (50 mg, 0.087 mmol) was mixed with K_2CO_3 (18 mg, 0.131 mmol) in MeCN (3.2 mL) and H_2O (1.6 mL). The vial was sealed and irradiated by microwaves to 100 °C for 25 min. H_2O (5 mL) and TFA (20 μL) was added to the reaction mixture to pH 2. The reaction mixture was thereafter extracted with EtOAc before the organic phase was evaporated. This was mixed with the N-deprotected HCl-salt of **3** (28.7 mg, 0.101 mmol), HATU (38.4 mg, 0.101 mmol), and DIEA (83 μL, 0.487 mmol) in dry DMF. The reaction was stirred for 4 h before EtOAc (20 mL) was added and the reaction mixture was washed with 0.1 M $NaHSO_4$ followed by 0.035 M $NaHSO_4$. Thereafter, the organic phase was evaporated. Purification on silica gel (CH_2Cl_2/MeOH 95:5) followed by purification and separation on preparative HPLC (MeCN/H_2O (0.1% TFA)) yielded the two diastereomers **22L** (3.96 mg, 6%) and **22D** (2.32 mg, 3.5%) as white solids. **22L** ^{1}H NMR (CD_3OD): δ 8.28–8.23 (m, 2H), 7.59–7.55 (m, 2H), 7.46–7.38 (m, 3H), 7.26–7.22 (m, 2H), 6.82 (dd, J = 10.6, 17.3 Hz, 1H), 6.61 (dd, J = 1.6, 17.3 Hz, 1H), 5.80 (m, 1H), 5.71 (dd, J = 1.6, 10.6 Hz, 1H), 5.67 (dd, J = 10.3, 17.1 Hz, 1H), 5.62 (s, 1H), 5.12–4.87 (m, 4H), 4.35 (m, 1H), 4.12–4.04 (m, 3H), 3.38–3.19 (m, 2H), 2.40–2.32 (m, 2H), 2.11–2.04 (m, 2H), 1.85–1.68 (m, 4H), 1.55–1.38 (m, 2H), 1.02 (s, 9H), 0.96 (t, J = 7.3 Hz, 3H). ^{13}C NMR (CD_3OD): δ 173.3, 172.7, 172.0, 171.8, 166.1, 165.3, 158.5, 153.9, 138.2, 137.7, 136.1, 135.3, 131.9, 130.2, 129.4, 129.3, 123.3, 122.8, 117.5, 116.6, 103.6, 65.3, 63.9, 57.4, 55.0, 53.0, 35.4, 34.5, 34.4, 32.8, 27.1, 23.4, 19.9, 13.9. HRMS calcd for $C_{41}H_{52}N_6O_8S$ $[M+H]^+$ 789.3646, found: 789.3649. HPLC purity (system 1: 100%, system 2: 100%). **22D** ^{1}H NMR (CD_3OD): δ 8.26–8.22 (m, 2H), 7.58–7.55 (m, 2H), 7.47–7.36 (m, 3H), 7.29–7.25 (m, 2H), 6.87 (s, 1H), 6.84 (dd, J = 10.5, 17.3 Hz, 1H), 6.63 (dd, J = 1.6, 17.3 Hz, 1H), 5.83 (m, 1H), 5.72 (dd, J = 1.6, 10.5 Hz, 1H), 5.56 (s, 1H), 5.14–4.94 (m, 4H), 4.32 (m, 1H), 4.17–4.01 (m, 3H), 3.45–3.29 (m, 2H), 2.42–2.34 (m, 2H), 2.19–2.11 (m, 2H), 1.94–1.68 (m, 4H), 1.41–1.26 (m, 2H), 0.99 (s, 9H), 0.88 (t, J = 7.3 Hz, 3H). ^{13}C NMR (CD_3OD): δ 173.2, 172.7, 171.9 (2 carbons), 166.3, 165.3, 158.7, 154.2, 138.5, 138.0, 136.3, 135.8, 135.5, 131.9, 130.7, 129.4, 129.3, 123.2, 123.1, 117.6, 116.6, 103.9, 65.5, 64.4, 58.3, 55.4, 53.1, 35.3, 34.6, 34.3, 32.9, 27.1, 23.6, 19.9, 13.9. HRMS calcd for $C_{41}H_{52}N_6O_8S$ $[M+H]^+$ 789.3646, found: 789.3638. HPLC purity (system 1: 100%, system 2: 100%).

7.1.27. Compound 23

In a microwave process vial, compound **11** (60 mg, 0.0885 mmol), was mixed with Hoveyda–Grubbs 2nd generation catalyst (14 mg, 0.0223 mmol) in trifluorotoluene (20 mL). The vial was sealed under N_2 and irradiated by microwaves to 110 °C for 5 min. After filtration, the solvent was evaporated. Purification on silica gel (CH_2Cl_2/MeOH 88:12) yielded **23** (24.4 mg, 43%) as a white solid. ^{1}H NMR (CD_3OD): δ 8.40–8.36 (m, 2H), 7.71–7.68 (m, 2H), 7.52–7.46 (m, 3H), 7.26–7.22 (m, 2H), 6.52 (d, J = 16.1 Hz, 1H), 6.34 (m, 1H), 6.29 (s, 1H), 5.38 (s, 1H), 4.38 (m, 1H), 3.27–3.22 (m, 2H), 2.47–2.40 (m, 2H), 1.96 (m, 1H), 1.90–1.79 (m, 2H), 1.72 (m, 1H), 1.46 (s, 9H), 0.98 (t, J = 7.3 Hz, 3H). ^{13}C NMR (CD_3OD): δ 174.7, 173.4, 172.2, 167.9, 166.7, 157.3, 153.9, 140.0, 138.3, 138.1, 132.1, 132.0, 130.2, 129.5 (2 carbons), 123.0, 98.6, 81.0, 58.8, 54.9, 52.4, 35.4, 31.0, 28.7, 23.2, 20.0, 14.0. MS calcd for $C_{33}H_{39}N_5O_7S$ $[M+H]^+$ 650.3, found: 650.0.

7.1.28. Compound 24

In two microwave process vials, compound **12** (70 mg, 0.10 mmol) was mixed with Hoveyda–Grubbs 2nd generation catalyst (4.4 mg, 0.0070 mmol) in trifluorotoluene (37.6 mL). The vials were sealed under N_2 and irradiated by microwaves to 100 °C for 7.5 min. After filtration, the reaction mixtures were pooled and evaporated. Purification on silica gel (CH_2Cl_2/MeOH 90:10) yielded

24 (7.3 mg, 11%) as a white solid. ^{1}H NMR (CD_3OD): δ 8.68 (dd, J = 1.2, 8.4 Hz, 1H), 8.38–8.35 (m, 2H), 8.22 (dd, J = 1.7, 8.0 Hz, 1H), 7.64 (m, 1H), 7.65–7.63 (m, 2H), 7.49–7.45 (m, 3H), 7.41 (ddd, J = 1.8, 7.3, 8.5 Hz, 1H), 7.33–7.26 (m, 2H), 7.05 (ddd, J = 1.3, 7.3, 8.1 Hz, 1H), 6.52 (d, J = 16.1 Hz, 1H), 6.48 (s, 1H), 5.48 (s, 1H), 3.06–2.94 (m, 2H), 2.52 (m, 1H), 2.37 (m, 1H), 2.01 (m, 1H), 1.88 (m, 1H), 1.47 (s, 9H). ^{13}C NMR (CD_3OD): δ 176.7, 173.0, 170.0, 168.5, 166.6, .4, 154.3, 141.6, 141.0, 138.4, 137.3, 132.9, 132.5, 132.0, 131.6, 129.5 (2 carbons), 123.6, 123.0, 122.9, 120.5, 99.2, 80.7, 60.7, 51.3, 31.4, 28.7, 24.2. MS calcd for $C_{35}H_{35}N_5O_7S$ $[M+H]^+$ 670.2, found: 670.4.

7.1.29. Compound 25

In eight microwave process vials, compound **14** (133.6 mg, 0.19 mmol) was mixed with Hoveyda–Grubbs 2nd generation catalyst (36.3 mg, 0.058 mmol) in trifluorotoluene (92 mL). The vials were sealed under N_2 and irradiated by microwaves to 110 °C. The reaction mixtures were pooled and evaporated. Purification on silica gel (CH_2Cl_2/MeOH 95:5 to 90:10) yielded **25** (31.4 mg, 28%). A small fraction was purified on HPLC (MeCN/H_2O with 25 mM NH_4OAc, pH 6.3). ^{1}H NMR (CD_3OD, NH_4^+-salt): δ 8.31 (m, 1H), 8.15–8.11 (m, 2H), 7.79 (m, 1H), 7.67 (s, 1H), 7.56–7.51 (m, 2H), 7.36 (m, 1H), 7.25–7.17 (m, 4H), 6.45 (d, J = 11.5 Hz, 1H), 6.02 (s, 1H), 5.70 (m, 1H), 5.24 (s, 1H), 4.04 (s, 3H), 3.69–3.63 (m, 2H), 2.54 (m,1H), 2.43 (m, 1H), 1.47 (s, 9H). ^{13}C NMR (CD_3OD): δ 174.5, 173.6, 172.5, 170.7, 164.9, 157.5, 152.2, 140.2, 137.8, 136.8, 132.9, 132.8, 132.2, 132.0, 131.5, 131.1, 129.2 (2 carbons), 129.1, 127.7, 126.7, 125.5, 124.1, 124.0, 121.3, 89.4, 81.1, 62.1, 54.7, 52.4, 28.7, 25.3. HRMS calcd for $C_{35}H_{35}N_5O_8S$ $[M+H]^+$ 686.2285, found: 686.2288. HPLC purity (system 1: 100%, system 2: 95.4%).

7.1.30. Compound 26

Prepared according to the general procedure C, using the N-deprotected TFA-salt of **23** (20.4 mg, 0.031 mmol), Boc-L-*t*Leu (14.2 mg, 0.062 mmol), HATU (28 mg, 0.074 mmol), DIEA (61 μL, 0.36 mmol) and DMF (1.5 mL). The reaction was stirred 2 h in room temperature. EtOAc (20 mL) was added, and the reaction mixture washed with 0.1 M $NaHSO_4$ follwed by 0.035 M $NaHSO_4$ before the organic phase was evaporated. Purification on preparative HPLC (MeCN/H_2O (0.05% HCOOH)) yielded **26** (14.3 mg, 61%) as a white solid. ^{1}H NMR (CD_3OD): δ 8.41–8.38 (m, 2H), 7.75–7.71 (m, 2H), 7.53–7.47 (m, 3H), 7.27–7.22 (m, 2H), 6.56 (d, J = 16.1 Hz, 1H), 6.36 (m, 1H), 6.32 (s, 1H), 5.63 (s, 1H), 4.40 (dd, J = 3.9, 10.0 Hz, 1H), 4.08 (s, 1H), 3.27–3.24 (m, 2H), 2.50–2.43 (m, 2H), 1.99 (m, 1H), 1.92–1.78 (m, 2H), 1.71 (m, 1H), 1.57–1.47 (m, 2H), 1.45 (s, 9H), 1.04 (s, 9H), 0.98 (t, J = 7.3 Hz, 3H). ^{13}C NMR (CD_3OD): δ 173.7, 173.4, 173.2, 171.9, 168.0, 166.7, 158.0, 154.0, 139.9, 138.4, 137.3, 132.2, 132.1, 130.5, 129.5 (2 carbons), 123.0, 98.6, 80.7, 63.7, 57.9, 54.5, 52.6, 35.4, 35.1, 31.0, 28.7, 27.2, 23.1, 20.1, 13.9. HRMS calcd for $C_{39}H_{50}N_6O_8S$ $[M+H]^+$ 763.3489, found: 763.3497. HPLC purity (system 1: 100%, system 2: 99.0%).

7.1.31. Compound 27

Prepared according to the general procedure C, using the N-deprotected TFA-salt of **24** (7.5 mg, 0.011 mmol), Boc-L-*t*Leu (5.0 mg, 0.022 mmol), HATU (9.9 mg, 0.026 mmol), DIEA (14.5 μL, 0.085 mmol), and DMF (1 mL). The reaction was stirred in room temperature for 3 h. EtOAc (10 mL) was added and the reaction mixture was washed with 0.1 M $NaHSO_4$ follwed by 0.035 M $NaHSO_4$ before the organic phase was evaporated. Purification on preparative HPLC (MeCN/H_2O (0.05% HCOOH)) yielded **27** (1.73 mg, 20%) as a white solid. ^{1}H NMR (CD_3OD): δ 8.68 (m, 1H), 8.41–8.37 (m, 2H), 7.98 (dd, J = 1.7, 7.9 Hz, 1H), 7.70–7.66 (m, 2H), 7.56–7.45 (m, 4H), 7.33–7.30 (m, 2H), 7.14 (m, 1H), 6.56 (d, J = 16.2 Hz, 1H), 6.50 (s, 1H), 6.42 (m, 1H), 5.76 (s, 1H), 4.03 (s, 1H), 3.54 (m, 1H), 3.20 (m, 1H), 2.55 (m, 1H), 2.44 (m, 1H), 2.09 (m, 1H), 1.91 (m, 1H), 1.44 (s, 9H), 1.04 (s, 9H). ^{13}C NMR (CD_3OD): δ 173.0, 172.9, 169.8, 168.4, 166.7, 157.9, 154.5, 141.4, 140.2, 138.4, 136.3, 134.4, 132.1, 131.9, 131.3, 129.5 (2 carbons), 124.1, 123.2, 123.1, 121.5, 99.3, 80.6, 63.7, 59.3, 52.1, 35.5, 31.1, 28.7, 27.2, 23.6. HRMS calcd for $C_{41}H_{46}N_6O_8S$ $[M+H]^+$ 783.3176, found: 783.3174. HPLC purity (system 1: 100%, system 2: 100%).

7.1.32. Compound 28

Prepared according to the general procedure C, using the N-deprotected TFA-salt of **25** (29.9 mg, 0.043 mmol), Boc-L-*t*Leu (19.8 mg, 0.085 mmol), HATU (39.0 mg, 0.102 mmol), DIEA (57 μL, 0.24 mmol), and DMF (2 mL). The reaction was stirred in room temperature for 2 h. Purification on preparative HPLC yielded **28** (11.7 mg, 33%) as the NH_4^+-salt. ^{1}H NMR (CD_3OD): δ 8.29 (d, J = 8.1 Hz, 1H), 8.12 (dd, J = 1.3, 8.1 Hz, 2H), 7.81 (m, 1H), 7.73 (s, 1H), 7.56–7.48 (m, 3H), 7.35 (m, 1H), 7.24–7.15 (m, 4H), 6.44 (d, J = 11.7 Hz, 1H), 6.02 (s, 1H), 5.71 (m, 1H), 5.52 (s, 1H), 4.12 (s, 1H), 4.03 (s, 3H), 3.74 (m, 1H), 3.48 (m, 1H), 2.59 (m, 1H), 2.36 (m, 1H), 1.43 (s, 9H), 1.08 (s, 9H). ^{13}C NMR (CD_3OD): δ 173.7, 173.4, 172.4, 170.0, 165.1, 157.9, 152.3, 139.6, 137.9, 136.0, 133.7, 132.1, 131.7, 131.2, 130.9, 129.3, 129.2, 128.5, 127.4, 124.7 (2 carbons), 124.1, 122.4, 89.5, 80.7, 63.5, 60.8, 54.7, 53.1, 35.5, 28.7, 27.3, 25.0. HRMS calcd for $C_{41}H_{48}N_6O_9S$ $[M+H]^+$ 799.3047, found; 799.3121. HPLC purity (system 1: 100%, system 2: 99.6%).

7.1.33. Compounds 29L, 29D and 30

Compound **17** (84.1 mg, 0.098 mmol) was lyophilized in CH_3CN and HCOOH (3.7 μL, 0.098 mmol). This was mixed with HCOOH (3.7 μL, 0.098 mmol), Hoveyda–Grubbs 2nd generation catalyst (6.1 mg, 0.0098 mmol) and trifluorotoluene (64 mL) in four microwave process vials. The vials were heated by microwaves to 100 °C for 5 min. The reactions were thereafter pooled and evaporated. Purification on silica gel (CH_2Cl_2/MeOH 90:10) followed by purification on preparative HPLC (MeCN/H_2O with 25 mM NH_4OAc, pH 6.3) yielded **29L** (9.15 mg, 11%), **29D** (4.93 mg, 6%), and **30** (2.24 mg, 3%) as the NH_4^+-salts. **29L** ^{1}H NMR (CD_3OD): δ 8.27 (m, 3H), 7.94 (m, 1H), 7.64 (d, J = 8.6 Hz, 2H), 7.46–7.36 (m, 4H), 7.26 (d, J = 8.6 Hz, 2H), 7.16 (m, 1H), 6.09 (s, 1H), 5.53 (s, 1H), 5.41–5.29 (m, 2H), 4.28 (m, 1H), 4.07 (s, 3H), 3.57 (m, 1H), 3.23 (m, 1H), 2.31–2.06 (m, 6H), 2.05 (m, 2H), 1.62 (m, 1H), 1.44 (s, 9H), 1.42–1.35 (m, 3H). ^{13}C NMR (CD_3OD): δ 176.3, 173.8, 172.6, 171.4, 165.3, 158.1, 154.6, 139.4, 138.1, 134.6, 133.5, 133.2, 132.1, 130.8, 130.6, 129.4 (2 carbons), 124.6, 123.1, 122.5, 121.2, 119.9, 90.0, 80.4, 61.4, 55.6, 54.7, 52.7, 33.5, 32.4, 32.0, 29.0, 28.8, 28.5, 26.3, 23.8. HRMS calcd for $C_{43}H_{50}N_6O_9S$ $[M+H]^+$ 827.3438, found: 827.3436. HPLC purity (system 1: 99.1%, system 2: 98.4%). **29D** ^{1}H NMR (CD_3OD): δ 8.43 (m, 1H), 8.27–8.22 (m, 2H), 7.94 (m, 1H), 7.57 (d, J = 8.8 Hz, 2H), 7.52 (ddd, J = 1.5, 7.4, 8.4 Hz, 1H), 7.46–7.36 (m, 3H), 7.27–7.23 (m, 2H), 7.19 (m, 1H), 6.09 (s, 1H), 5.57 (s, 1H), 5.42–5.29 (m, 2H), 4.07 (s, 3H), 4.04 (m, 1H), 3.59 (m, 1H), 3.23 (m, 1H), 2.27–2.22 (m, 2H), 2.07–1.97 (m, 4HV), 1.92–1.83 (m, 2H), 1.51 (m, 1H), 1.38 (s, 9H), 1.33–1.24 (m, 3H). ^{13}C NMR (CD_3OD): J = 176.5, 173.8, 172.6, 171.0, 165.3, 157.8, 154.6, 139.7, 138.1, 134.9, 133.8, 133.5, 132.1, 131.0, 130.8, 130.6, 129.4 (2 carbons), 124.7, 124.1, 123.0, 122.3, 90.1, 80.8, 60.7, 58.0, 54.7, 52.9, 33.8, 32.3, 31.9, 28.8, 28.7, 28.6, 26.4, 24.0. HRMS calcd for $C_{43}H_{50}N_6O_9S$ $[M+H]^+$ 827.3438, found: 827.3441. HPLC purity (system 1: 100%, system 2: 96.6%). Compound **30** ^{1}H NMR (CD_3OD, major isomer reported): δ 8.38 (m, 1H), 8.27–8.23 (m, 2H), 7.98 (m, 1H), 7.64–7.58 (m, 2H), 7.52–7.36 (m, 4H), 7.28–7.22 (m, 2H), 7.18 (m, 1H), 6.10 (s, 1H), 5.58 (s, 1H), 5.41–5.33 (m, 2H), 4.25 (m, 1H), 4.07 (s, 3H), 3.60 (m, 1H), 3.26 (m, 1H), 2.59 (m, 1H), 2.23–2.15 (m, 2H), 2.07–1.89 (m, 6H), 1.70 (m, 1H), 1.40 (s, 9H). HRMS calcd for $C_{42}H_{48}N_6O_9S$ $[M+H]^+$ 813.3282, found: 813.3284. HPLC purity (system 1: 100%, system 2: 98.1%).

7.1.34. Compounds 31L, 31D and 32

Mixed fractions from the purification of **29** (7.4 mg, 0.0089 mmol), and Pd/C (10%) (2 mg, 0.0009 mmol) was mixed in THF (4 mL). The reaction was stirred under H_2-atmosphere for 27 h. Filtration followed by purification on preparative HPLC (MeCN/H_2O with 25 mM NH_4OAc, pH 6.3) yielded **31L** (1.02 mg, 14%), **31D** (0.86 mg, 12%), and **32** (1.13 mg, 15%) as the NH_4^+-salts. **31L** ^{1}H NMR (CD_3OD): δ 8.26–8.23 (m, 2H), 8.15 (d, J = 8.4 Hz, 1H), 7.72 (d, J = 8.5 Hz, 1H), 7.61–7.56 (m, 3H), 7.46–7.35 (m, 3H), 6.04 (s, 1H), 5.52 (s, 1H), 4.25 (m, 1H), 4.06 (s, 3H), 6.04 (s, 1H), 5.52 (s, 1H), 4.25 (m, 1H), 4.06 (s, 3H), 3.63 (m, 1H), 3.50 (m, 1H), 1.99–1.88 (m, 3H), 1.66 (m, 1H), 1.61–1.50 (m, 2H), 1.41 (s, 9H), 1.35–1.24 (m, 12H). HRMS calcd for $C_{43}H_{52}N_6O_9S$ $[M+H]^+$ 829.3595, found: 829.3593. HPLC purity (system 1: 100%, system 2: 100%). Compound **31D** (CD_3OD): δ 8.27–8.23 (m, 2H), 8.16 (m, 1H), 7.85 (m, 1H), 7.62–7.58 (m, 2H), 7.54 (m, 1H), 7.46–7.36 (m, 4H), 7.28–7.20 (m, 3H), 6.11 (s, 1H), 5.59 (s, 1H), 4.13 (m, 1H), 4.07 (s, 3H), 3.56 (m, 1H), 3.26 (m, 1H), 1.97–1.90 (m, 2H), 1.86–1.71 (m, 3H), 1.59–1.51 (m, 2H), 1.39 (s, 9H), 1.35–1.28 (m, 5H). HRMS calcd for $C_{43}H_{52}N_6O_9S$ $[M+H]^+$ 829.3595, found: 829.3593. HPLC purity (system 1: 100%, system 2: 100%). Compound **32** ^{1}H NMR (CD_3OD): δ 8.27–8.23 (m, 2H), 8.08 (m, 1H), 7.87 (m, 1H), 7.67–7.62 (m, 2H), 7.50 (m, 1H), 7.45–7.35 (m, 4H), 7.27–7.23 (m, 2H), 7.20 (m, 1H), 6.10 (s, 1H), 5.60 (s, 1H), 4.16 (m, 1H), 4.07 (s, 3H), 3.48 (m, 1H), 3.26 (m, 1H), 1.97–1.90 (m, 2H), 1.80–1.72 (m, 2H), 1.58–1.49 (m, 2H), 1.39 (s, 9H), 1.37–1.34 (m, 4H). HRMS calcd for $C_{42}H_{50}N_6O_9S$ $[M+H]^+$ 815.3438, found: 815.3447. HPLC purity (system 1: 100%, system 2: 100%).

7.1.35. Compound 33

In a microwave process vial, **21** (21.5 mg, 0.0375 mmol) and Hoveyda–Grubbs 2nd generation catalyst (1.6 mg, 0.0026 mmol) were mixed in trifluorotoluene (18.5 mL). The vial was sealed under N_2 and irradiated by microwaves to 110 °C for 5 min. The reaction mixtures were pooled and filtrated on a small plug of RP silica gel before evaporation. Purification on silica gel (EtOAc/*i*-hexane 2:3) yielded **33** (13.9 mg, 68%) as a white solid. ^{1}H NMR ($CDCl_3$): δ 8.49–8.46 (m, 2H), 7.50–7.45 (m, 5H), 7.22–7.15 (m, 2H), 7.06 (d, J = 6.8 Hz, 1H), 6.56 (d, J = 16.3 Hz, 1H), 6.16 (m, 1H), 6.04 (s, 1H), 5.56 (d, J = 7.3 Hz, 1H), 5.35 (d, J = 9.7 Hz, 1H), 4.50 (m, 1H), 3.91–3.85 (m, 2H), 3.81 (s, 3H), 2.63 (m, 1H), 2.47 (m, 1H), 1.02 (s, 9H). ^{13}C NMR ($CDCl_3$): δ 171.9, 170.8, 169.9, 166.4, 165.6, 156.4, 152.8, 137.0, 135.9, 135.8, 131.4, 131.1, 128.6 (2 carbons), 96.8, 63.6, 63.1, 56.2, 53.5, 34.6, 32.0, 26.4. MS calcd for $C_{30}H_{32}N_4O_6$ $[M+H]^+$ 545.2, found: 545.0.

7.1.36. Compound 34

In a microwave process vial, **33** (14.8 mg, 0.027 mmol) was mixed with K_2CO_3 (5.5 mg, 0.040 mmol) in MeCN (1.5 mL) and H_2O (5 mL). The vial was sealed and irradiated by microwaves to 100 °C for 15 min. H_2O (3 mL) and TFA (10 μL) was added to the reaction mixture to pH 2. The reaction mixture was thereafter extracted with EtOAc before the organic phase was evaporated. This was mixed with the N-deprotected HCl-salt of **2** (9.4 mg, 0.031 mmol), HATU (11.7 mg, 0.031 mmol), DIEA (25.4 μL, 0.15 mmol) in dry DCM. The reaction was stirred at 45 °C for 2 h. CH_2Cl_2 (6 mL) was added and the reaction mixture was washed with 0.1 M $NaHSO_4$ followed by 0.035 M $NaHSO_4$ before the organic phase was evaporated. Purification by preparative HPLC (MeCN/H_2O (0.1% TFA)) yielded **34** (9.0 mg, 45%). ^{1}H NMR ($CDCl_3$): δ 11.06 (s, 1H), 8.61 (m, 1H), 8.44–8.40 (m, 2H), 7.65–7.60 (m, 3H), 7.52–7.43 (m, 6H), 7.17 (m, 1H), 6.62 (d, J = 16.9 Hz, 1H), 6.22 (m, 1H), 6.11 (s, 1H), 5.77 (m, 1H), 5.61 (d, J = 6.2 Hz, 1H), 5.45 (d, J = 9.6 Hz, 1H), 5.15–5.06 (m, 2H), 4.50 (m, 1H), 3.97 (m, 1H), 3.88 (m, 1H), 3.55–3.41 (m, 2H), 2.65 (m, 1H), 2.48 (m, 1H), 2.29–2.22 (m, 2H), 2.01–1.88 (m, 2H), 1.04 (s, 9H). ^{13}C NMR ($CDCl_3$): δ 172.0, 170.1, 167.8, 167.7, 165.8, 165.3, 156.5, 152.8, 140.3, 137.0, 136.5, 136.1, 135.6, 133.2, 131.6, 130.3, 128.8, 128.7, 128.2, 127.8, 124.1, 123.4, 122.1, 117.0, 116.8, 96.9, 63.6, 63.2, 58.1, 53.3, 34.5, 32.1, 31.9, 26.5, 22.4. HRMS calcd for $C_{41}H_{44}N_6O_8S$ $[M+H]^+$ 781.3020, found: 781.3017.

7.1.37. Compound 35

In a microwave process vial, compound **33** (5.0 mg, 0.009 mmol) was mixed with K_2CO_3 (1.9 mg, 0.014 mmol) in MeCN (0.5 mL) and H_2O (0.25 mL). The vial was sealed and irradiated by microwaves to 100 °C for 15 min. H_2O (1 mL) and TFA (10 μL) was added to the reaction mixture to pH 2. The reaction mixture was thereafter extracted with EtOAc before evaporation of the organic phase. This was mixed with the N-deprotected HCl-salt of **3** (1.54 mg, 0.010 mmol), HATU (3.8 mg, 0.010 mmol), DIEA (8.4 μL, 0.05 mmol) in dry DMF (0.25 mL). The reaction was stirred in room temperature for 1 h. EtOAc was added and the reaction mixture was washed with sodium acetate buffer pH 4 before evaporation of the organic phase. Purification on preparative HPLC (MeCN/H_2Ob (0.1% TFA)) yielded **35** (2.1 mg, 32%) as a white solid. ^{1}H NMR (CD_3OD): δ 8.40–8.37 (m, 2H), 7.70–7.64 (m, 2H), 7.53–7.47 (m, 3H), 7.22–7.19 (m, 2H), 6.57 (d, J = 16.4 Hz, 1H), 6.33 (m, 1H), 6.19 (s, 1H), 5.67 (m, 1H), 5.63 (s, 1H), 5.09–4.09 (m, 2H), 4.48 (m, 1H), 4.37 (m, 1H), 4.08 (s, 1H), 3.87 (m, 1H), 3.28–3.25 (m, 2H), 2.66 (m, 1H), 2.52 (m, 1H), 2.20–2.14 (m, 2H), 1.89–1.81 (m, 2H), 1.79–1.64 (m, 2H), 1.51–1.37 (m, 2H), 1.01 (s, 9H), 0.97 (t, J = 7.4 Hz, 3H). ^{13}C NMR (CD_3OD): δ 173.6, 173.2, 172.1, 171.3, 171.0, 167.7, 166.7, 158.4, 153.8, 139.0, 138.3, 138.1, 138.0, 132.2, 131.5, 129.6, 129.5, 116.7, 97.9, 88.3, 64.5, 63.7, 57.0, 55.2, 53.1, 35.1, 34.4, 33.5, 32.9, 26.9, 23.6, 20.1, 14.0. HRMS calcd for $C_{39}H_{48}N_6O_8S$ $[M+H]^+$ 761.3333, found: 761.3336. HPLC purity (system 1: 100%, system 2: 98.7%).

7.1.38. Compound 36 (2-((*tert*-butoxycarbonyl)amino)-2-(4-((7-methoxy-2-phenylquinolin-4-yl)oxy)-3-vinylphenyl)acetic acid)

Prepared as described previously by us.[31]

7.1.39. Compound 37

Prepared according to the general procedure, using **36** (54.5 mg, 0.103 mmol), the N-deprotected HCl-salt of **2** (31.4 mg, 0.103 mmol), HATU (62.7 mg, 0.165 mmol) and DIEA (154 μL, 0.886 mmol). The reaction was stirrred for 3.5 h. Purification on silica gel (CH_2Cl_2/MeOH 93:7) gave **37** (39.5 mg, 50%) as a white solid. ^{1}H NMR (CD_3OD): δ 8.45 (m, 1H), 8.21 (d, J = 9.2 Hz, 1H), 8.11 (m, 1H), 7.99 (d, J = 2.3 Hz, 1H), 7.72–7.76 (m, 2H), 7.63 (dd, J = 2.3, 8.5 Hz, 1H), 7.44 (d, J = 2.5 Hz, 1H), 7.41–7.28 (m, 4H), 7.20 (dd, J = 2.5, 9.1 Hz, 1H), 7.14 (d, J = 8.4 Hz, 1H), 6.99 (m, 1H), 6.72 (dd, J = 11.6, 18.0 Hz, 1H), 6.62 (s, 1H), 5.96 (d, J = 18.0 Hz, 1H), 5.66 (m, 1H), 5.38 (s, 1H), 5.22 (d, J = 11.8 Hz, 1H), 4.94–4.80 (m, 2H), 3.95 (s, 3H), 3.30–3.16 (m, 2H), 2.08–1.99 (m, 2H), 1.91–1.79 (m, 2H), 1.45 (s, 9H). ^{13}C NMR (CD_3OD): δ 173.9, 170.9, 164.0, 163.6, 160.7, 152.1, 143.9, 141.4, 140.7, 140.1, 138.6, 138.5, 137.2, 133.2, 132.2, 130.7, 130.1, 129.8, 128.6, 127.9, 124.8, 123.9, 123.5, 121.1, 120.2, 118.4, 116.1, 115.8, 107.3, 106.2, 101.9, 81.1, 61.7, 56.1, 40.6, 38.9, 33.4, 28.7, 24.1. MS calcd for $C_{43}H_{44}N_4O_8S$ $[M+H]^+$ 777.3, found: 777.4.

7.1.40. Compound 38L and 38D

Prepared according to the general procedure C, using the N-deprotected HCl-salt of **37** (42 mg, 0.059 mmol), Boc-L-*t*Leu (21.9 mg, 0.095 mmol), HATU (27.0 mg, 0.071 mmol) and DIEA (89 μL, 0.51 mmol) the reaction was stirred in DMF for 1 h. Purification and separation of the diastereomers was performed on RP-HPLC (MeCN/H_2O (0.05% HCOOH)) giving compounds **38L** (5.1 mg, 10%) and **38D** (5.3 mg, 10%) as white solids. Compound

38L ^{1}H NMR (CD_3OD): δ 8.77 (m, 1H), 8.41 (d, J = 9.3 Hz, 1H), 8.17 (m, 1H), 8.02 (d, J = 2.8 Hz, 1H), 7.82 (m, 1H9, 7.72 (dd, J = 1.5, 6.9 Hz, 2H), 7.67 (m, 1H), 7.55 (d, J = 2.4 Hz, 1H), 7.53–7.48 (m, 2H), 7.46–7.39 (m, 2H), 7.32 (d, J = 8.6 Hz, 1H), 7.21 (dt, 1.4, 7.5 Hz, 1H), 6.78 (s, 1H), 6.77 (dd, J = 11.1, 17.8 Hz, 1H) 6.53 (m, 1H), 6.04 (m, 1H), 5.77–5.63 (m, 2H), 5.34 (dd, J = 1.2, 11.1 Hz, 1H), 5.01–4.70 (m, 2H), 4.04 (s, 3H), 3.36–3.17 (m, 2H), 2.12–2.05 (m, 2H), 1.87–1.77 (m, 2H), 1.40 (s, 9H), 1.04 (s, 9H). HPLC purity (system 1: 100%, system 2: 99.5%). Compound **38D** ^{1}H NMR (CD_3OD): δ 8.76 (m, 1H), 8.38 (d, J = 9.0 Hz, 1H), 8.12 (d, J = 8.1 Hz, 1H), 8.00 (d, J = 2.5 Hz, 1H), 7.80 (dd, J = 8.0, 1.7 Hz, 1H), 7.76–7.72 (m, 2H), 7.63 (dd, J = 2.2, 8.4 Hz, 1H), 7.55–7.40 (m, 5H), 7.37 (dd, J = 2.4, 9.1 Hz, 1H), 7.31 (d, J = 8.5 Hz, 1H), 7.22 (dt, 1.1, 7.6 Hz, 1H), 6.80 (dd, 11.3, 17.7 Hz, 1H), 6.72 (s, 1H), 6.03 (d, J = 18.1, 1H), 5.78–5.65 (m, 2H), 5.33 (dd, J = 1.2, 11.1 Hz, 1H), 4.95(m, 1H), 4.06 (s, 1H), 4.03 (s, 3H), 3.39–3.32 (m, 2H), 2.13–2.04 (m, 2H), 1.89–1.79 (m, 2H), 1.41 (s, 9H), 0.98 (s, 9H). HPLC purity (system 1: 100%, system 2: 99.7%). HRMS calcd for $C_{49}H_{55}N_5O_9S$ $[M+H]^+$ 890.3799, found: 890.3801 (on a mixture of **38L** and **38D**).

7.2. Enzyme Inhibition

The protease activity of the full-length HCV NS3/4A protein (protease–helicase/NTPase from genotype 1a was measured using a FRET-assay as described previously.[52,65] In short, 1nM enzyme was incubated for 10 min at 30 °C in 50 mM HEPES, pH 7.5, 10 mM DDT, 40% glycerol, 0.1% *n*-octyl-β-D-glucoside, 3.3% DMSO with 25 μM of the peptide cofactor 2K-NS4A (KKGSVVIVGRIVLSGK), and inhibitor. The reaction was started by the addition of 0.5 μM substrate (Ac-DED(Edans)EEAbuψ[COO]ASK(Dabcyl)-NH_2) obtained from AnaSpec Inc. (San Jose, USA). Non-linear regression analysis of the data was made using Grafit 5.0.13 (Erithacus software limited).

7.3. In silico predictions

The predicted pK_a and log$D_{7.4}$ values for compounds **13**, **15**, **17**, **18**, **19**, **29L** and **29D** were calculated using ADMET predictor v.5.5 and are presented in Table 8 in the manuscript.

7.4. In vitro preclinical profiling

7.4.1. Metabolic stability

The Cl_{int} can be used predictively as measurement of the in vivo metabolic stability when the total clearance mechanism can be described as hepatic and metabolic, and when oxidative metabolism dominates. Compounds **13**, **15**, **17**, **18**, **19**, **29L** and **29D** (1 μM) were pre-incubated for 5 min at 37 °C with pooled human liver microsomes (0.5 mg/mL; Xenotech, Kansas, KS) in 0.1 M potassium phosphate buffer pH 7.4 prior to the addition of NADPH (1 mM final concentration) to initiate the reaction. The reaction was then incubated for 0, 5, 15 and 40 min and at each time point the reaction was quenched by addition of ice-cold acetonitrile (35% final concentration) containing 0.1 μM Warfarin as an internal standard. Plates were centrifuged at 3500 rpm for 20 min at 4 °C, and the supernatants were subjected to LC/MS/MS.

The natural logarithm of the analytical peak area ratio (relative to 0 min sample which was considered as 100%) was plotted against time and analyzed by linear regression. In vitro half-life ($t_{1/2}$) and in vitro intrinsic clearance (Cl_{int}) were calculated on the basis of first-order reaction kinetics of the percentage of remaining compound according to previously published models.[55,56] Dextromethorphan (3 μM) and Midazolam (5 μM) were used as positive controls for cytochrome P450 enzymes (CYP) isoforms CYP2D6 and CYP3A4, respectively. The cut-off values that were used to classify the compounds regarding metabolic stability follows: Cl_{int} <47 (μl/min/mg) indicates a low risk for high first metabolism in vivo, 47 < Cl_{int} < 92 a moderate risk, and Cl_{int} >92 a high risk.

7.4.2. Solubility determinations

Determination of solubility was performed by addition of an aliquot of DMSO stock (10 mM) to phosphate buffered saline (PBS) (final DMSO concentration 1%). Incubation with rotation in HPLC glass vials for for 2 h at 37 °C. The samples were then centrifuged at 10,000×g for 30 min and the supernatant analyzed with LC–MS/MS. This medium throughput method can thus only detect solubilities below 100 μM.

7.4.3. Cell culture

Caco-2 cells, obtained from American Tissue Collection, Rockville, MD, were maintained in an atmosphere of 90% air and 10% CO_2, as described previously.[57] For transport experiments, 3.0×10^5 cells were seeded on polycarbonate filter inserts (12 mm diameter; pore size 0.4 μm; Costar, Cambridge, MA) and allowed to grow and differentiate for 21–24 days. The monolayers integrity was assessed by measuring the paracellular marker [^{14}C]-Mannitol (1.0 μCi/mmol; Perkin–Elmer Life Sciences, Boston, MA) transport and the transepithelial electrical resistance (TEER) before and after the experiments.

7.4.4. Permeability experiments

Stock solutions (10 mM) of the compounds were prepared in DMSO and diluted to 10 μM (final DMSO concentration of 0.1%) in fasted state simulated intestinal fluid (FASSIF) at pH 7.4. HBSS pH 7.4 supplemented with 1% (w/v) BSA was prepared to be used in the receiving, basolateral, compartment.

The Caco-2 study was performed in accordance with published protocols.[57] Caco-2 cell monolayers (passage 94–105) were grown on permeable filter support and used for transport study on day 21 after seeding. Prior to the experiment a drug solution of 10 μM was prepared and warmed to 37 °C. The Caco-2 filters were washed with pre-warmed Hank's balanced salt solution (HBSS) prior to the experiment, and thereafter the experiment was started by applying the donor solution on the apical side. The experiments were performed at 37 °C and with a stirring rate of 500 rpm. The receiver compartment was sampled at 15, 30 and 60 min, and at 60 min also a final sample from the donor chamber was taken in order to calculate the mass balance of the compound. Directly after the termination of the experiment the filter inserts were washed with pre-warmed HBSS and the membrane integrity was checked. This was performed by transepithelial electrical resistance (TEER) measurement and by measurement of Mannitol permeability, which is a paracellular marker used for integrity measurements.

For transport studies performed under sink conditions, where less than 10% of the compound was transported across the Caco-2 cell monolayers, the apparent permeability coefficients (P_{app}) were calculated from the equation

$$P_{app} = \frac{\Delta Q}{\Delta t} \times \frac{1}{AC_0}$$

Where $\frac{\Delta Q}{\Delta t}$ is the steady-state flux (mol/s), C_0 is the initial concentration in the donor chamber at each time interval (mol/mL), and A is the surface area of the filter (cm^2). P_{app} was obtained from nonlinear regression of the accumulated dose in the receiver compartment over time, minimizing the sum of squared residuals in the equation.

A P_{app} value below 0.2×10^{-6} cm/s indicates low permeability, a P_{app} value between 0.2×10^{-6} cm/s to 1.6×10^{-6} cm/s indicates moderate permeability, and a P_{app} value above 1.6×10^{-6} cm/s indicates high permeability.[60]

Table 9
Mass spectrometric specific settings used for detection

Compound	ESI (±)	*m/z* (parent)	*m/z* (product)	Cone voltage (V)	Collision energy (V)
13	+	702.4	646.3	22	16
15	+	728.4	672.3	24	16
17	+	855.5	755.4	20	18
18	+	815.4	715.4	20	16
19	+	841.5	741.4	22	18
29L	+	827.5	727.4	20	18
29D	+	827.5	727.4	20	18

Radioactive samples ([^{14}C]-Mannitol) were analyzed with a liquid scintillation counter (TopCount NXT, Perkin–Elmer Life Sciences, Boston).

7.4.5. Data analysis

All experiments were performed in, at least, triplicates, and samples were subjected to liquid chromatography/mass spectrometry analysis with a Waters XEVO TQ triple-quadrupole mass spectrometer (electrospray ionization, ESI) coupled to a Waters Acquity UPLC (Waters Corp.). For chromatographic separation a general gradient was used (1% mobile phase B to 90% over 2.5 min total run) on a C18 BEH 1.7 μm column 2 × 50 mm (Waters Corp.). Mobile phase A consisted of 5% acetonitrile 0.1% formic acid and mobile phase B 100% acetonitrile 0.1% formic acid. The flow rate was 0.5 mL/min. 5 μL of the sample were injected onto a 10 μL loop in partial injection mode using the MS settings in Table 9. In general, a standard curve between 1–1000 nM was prepared for quantization. Warfarin was used as an internal standard in all samples.

7.5. Computational methodology

The crystal structure (pdb code 1CU1)[14] was prepared using the *Protein Preparation Wizard* implemented in Maestro (Schrödinger 2011). The A subunit was deleted and the B subunit was used in all modeling studies. Hydrogen's were added, correct bond orders assigned and crystallographic water molecules were deleted. The active site was made available for the docking studies by the deletion of the terminal residues (624–631) and Met623 was capped with an *N*-methyl group. The structure was minimized using restrained minimization with the OPLS-2005 force field and normal BatchMin cutoffs. Finally, the truncated protein structure that included only amino acids within 12 Å from residues 624–631 was created for docking studies.

To account for the conformational changes in the protein arising from the substitutions, induced fit docking was carried out using FLO (QXP 200605).[66] Protein flexibility was accounted for by allowing crucial amino acid residues in the binding pocket to move freely up to 0.2 Å. Movements larger than 0.2 Å were penalized by 20.0 kJ/mol/Å^2. Flexible residues occupying the active site, that is, Arg155, Gln526 and Lys136 were given full conformational freedom. Hydrogen bond constraints were applied between the inhibitors and the protein to restrict their translation away from the active site. These constraints mimic the hydrogen bond pattern found between the bound cleavage product and the protein. Four hydrogen bond constraints were used: between NH of Ala 157 and the backbone carbonyl oxygen of P3 substituent, between the backbone carbonyl oxygen of Arg155 and NH of the P1 substituent, and between the NHs of Gly137 and Ser139 and the corresponding carbonyl oxygen of the P1. For each inhibitor, 10 unique binding poses were generated using 6000 Monte Carlo perturbation cycles (mcldock). These poses were further subjected to 20 steps of simulated annealing followed by energy minimization. Each cycle involved 400 rapid Monte Carlo steps generating unique conformations within an energy window of 50 kJ/mol/Å and an RMSD >0.5 Å. Each of the complexes was submitted to a 3 fs dynamics at 600 K after 3000 fs of equilibration steps. The maximum movement of an atom in any single step was limited to 0.1 Å. Hydrogen vibrations were damped by assigning an atomic weight of 10 to the hydrogens. Among the 10 best poses generated, the most plausible binding mode conformation for each compound was selected based on visual inspection.

Acknowledgements

We gratefully acknowledge support from Swedish Research Council (grant nos. 9478, 21386 and D0571301), Knut and Alice Wallenberg's foundation, Science for Life Laboratory and Chemical Biology Consortium of Sweden (CBCS). We also thank Simulations Plus for providing access to the ADMET Predictor software, Johanna Grandin and Gunnar Lindeberg for technical support and Dr Aleh Yahorau, Department of Pharmaceutical Biosciences, Uppsala University, for help with HRMS analyzes and Medivir AB, Huddinge, Sweden for EC_{50}-determinations and financial support.

References

1. World Health Organization Homepage, http://www.who.int/mediacentre/factsheets/fs164/en/ (accessed May 2014), Hepatitis C, Fact Sheet No. 164. Last updated July 2013.
2. Brown, R. S. *Nature* **2005**, *436*, 973.
3. Vermehren, J.; Sarrazin, C. *Clin. Microbiol. Infect.* **2011**, *17*, 122.
4. Feld, J. J.; Hoofnagle, J. H. *Nature* **2005**, *436*, 967.
5. Malcolm, B. A.; Liu, R.; Lahser, F.; Agrawal, S.; Belanger, B.; Butkiewicz, N.; Chase, R.; Gheyas, F.; Hart, A.; Hesk, D.; Ingravallo, P.; Jiang, C.; Kong, R.; Lu, J.; Pichardo, J.; Prongay, A.; Skelton, A.; Tong, X.; Venkatraman, S.; Xia, E.; Girijavallabhan, V.; Njoroge, F. G. *Antimicrob. Agents Chemother.* **2006**, *50*, 1013.
6. Perni, R. B.; Almquist, S. J.; Byrn, R. A.; Chandorkar, G.; Chaturvedi, P. R.; Courtney, L. F.; Decker, C. J.; Dinehart, K.; Gates, C. A.; Harbeson, S. L.; Heiser, A.; Kalkeri, G.; Kolaczkowski, E.; Lin, K.; Luong, Y.; Rao, B. G.; Taylor, W. P.; Thomson, J. A.; Tung, R. D.; Wei, Y.; Kwong, A. D.; Lin, C. *Antimicrob. Agents Chemother.* **2006**, *50*, 899.
7. Ramachandran, P.; Fraser, A.; Agarwal, K.; Austin, A.; Brown, A.; Foster, G. R.; Fox, R.; Hayes, P. C.; Leen, C.; Mills, P. R.; Mutimer, D. J.; Ryder, S. D.; Dillon, J. F. *Aliment. Pharmacol. Ther.* **2012**, *35*, 647.
8. Rosenquist, Å.; Samuelsson, B.; Johansson, P.-O.; Cummings, M. D.; Lenz, O.; Raboisson, P.; Simmen, K.; Vendeville, S.; de Kock, H.; Nilsson, M.; Horvath, A.; Kalmeijer, R.; de la Rosa, G.; Beumont-Mauviel, M. *J. Med. Chem* **2014**, *57*, 1673.
9. Asselah, T. *Expert Opin. Pharmacother.* **2014**, *15*, 121.
10. Sarrazin, C.; Zeuzem, S. *Gastroenterology* **2010**, *138*, 447.
11. Ali, A.; Aydin, C.; Gildemeister, R.; Romano, K. P.; Cao, H.; Özen, A.; Soumana, D.; Newton, A.; Petropoulos, C. J.; Huang, W.; Schiffer, C. A. *ACS Chem. Biol.* **2013**, *8*, 1469.
12. Grakoui, A.; Wychowski, C.; Lin, C.; Feinstone, S. M.; Rice, C. M. *J. Virol.* **1993**, *67*, 1385.
13. Lindenbach, B. D.; Rice, C. M. *Nature* **2005**, *436*, 933.
14. Yao, N.; Reichert, P.; Taremi, S. S.; Prosise, W. W.; Weber, P. C. *Structure* **1999**, *7*, 1353.
15. Gale, M., Jr.; Foy, E. M. *Nature* **2005**, *436*, 939.
16. Llinàs-Brunet, M.; Bailey, M.; Fazal, G.; Goulet, S.; Halmos, T.; Laplante, S.; Maurice, R.; Poirier, M.; Poupart, M.-A.; Thibeault, D.; Wernic, D.; Lamarre, D. *Bioorg. Med. Chem. Lett.* **1998**, *8*, 1713.
17. Steinkuhler, C.; Biasiol, G.; Brunetti, M.; Urbani, A.; Koch, U.; Cortese, R.; Pessi, A.; De Francesco, R. *Biochemistry* **1998**, *37*, 8899.
18. Rönn, R.; Sandström, A. *Curr. Top. Med. Chem.* **2008**, *8*, 533.
19. Rönn, R.; Sabnis, Y. A.; Gossas, T.; Åkerblom, E.; Danielson, U. H.; Hallberg, A.; Johansson, A. *Bioorg. Med. Chem.* **2006**, *14*, 544.
20. Johansson, A.; Poliakov, A.; Åkerblom, E.; Wiklund, K.; Lindeberg, G.; Winiwarter, S.; Danielson, U. H.; Samuelsson, B.; Hallberg, A. *Bioorg. Med. Chem.* **2003**, *11*, 2551.
21. Poliakov, A.; Sandström, A.; Åkerblom, E.; Danielson, U. H. *J. Enzyme Inhib. Med. Chem.* **2007**, *22*, 191.
22. Lamarre, D.; Anderson, P. C.; Bailey, M.; Beaulieu, P.; Bolger, G.; Bonneau, P.; Bös, M.; Cameron, D. R.; Cartier, M.; Cordingley, M. G.; Faucher, A.-M.; Goudreau, N.; Kawai, S. H.; Kukolj, G.; Lagacé, L.; LaPlante, S. R.; Narjes, H.; Poupart, M.-A.; Rancourt, J.; Sentjens, R. E.; George, R., St.; Simoneau, B.; Steinmann, G.; Thibeault, D.; Tsantrizos, Y. S.; Weldon, S. M.; Yong, C.-L.; Llinàs-Brunet, M. *Nature* **2003**, *426*, 186.
23. Goudreau, N.; Llinàs-Brunet, M. Expert Opin. Investig *Drugs* **2005**, *14*, 1129.
24. Vanwolleghem, T.; Meuleman, P.; Libbrecht, L.; Roskams, T.; De Vos, R.; Leroux-Roels, G. *Gastroenterology* **2007**, *133*, 1144.

25. Liverton, N. J.; Carroll, S. S.; Dimuzio, J.; Fandozzi, C.; Graham, D. J.; Hazuda, D.; Holloway, M. K.; Ludmerer, S. W.; McCauley, J. A.; McIntyre, C. J.; Olsen, D. B.; Rudd, M. T.; Stahlhut, M.; Vacca, J. P. *Antimicrob. Agents Chemother.* **2010**, *54*, 305.
26. McCauley, J. A.; McIntyre, C. J.; Rudd, M. T.; Nguyen, K. T.; Romano, J. J.; Butcher, J. W.; Gilbert, K. F.; Bush, K. J.; Holloway, M. K.; Swestock, J.; Wan, B. L.; Carroll, S. S.; DiMuzio, J. M.; Graham, D. J.; Ludmerer, S. W.; Mao, S. S.; Stahlhut, M. W.; Fandozzi, C. M.; Trainor, N.; Olsen, D. B.; Vacca, J. P.; Liverton, N. J. *J. Med. Chem.* **2010**, *53*, 2443.
27. White, P. W.; Llinàs-Brunet, M.; Amad, M.; Bethell, R. C.; Bolger, G.; Cordingley, M. G.; Duan, J.; Garneau, M.; Lagacé, L.; Thibeault, D.; Kukolj, G. *Antimicrob. Agents Chemother.* **2010**, *54*, 4611.
28. Thompson, A. J.; Locarnini, S. A.; Beard, M. R. *Curr. Opin. Virol.* **2011**, *1*, 599.
29. Kieffer, T. L.; Kwong, A. D.; Picchio, G. R. *J. Antimicrob. Chemother.* **2010**, *65*, 202.
30. Örtqvist, P.; Peterson, S. D.; Åkerblom, E.; Gossas, T.; Sabnis, Y. A.; Fransson, R.; Lindeberg, G.; Danielson, U. H.; Karlén, A.; Sandström, A. *Bioorg. Med. Chem.* **2007**, *15*, 1448.
31. Lampa, A.; Ehrenberg, A. E.; Gustafsson, S. S.; Vema, A.; Åkerblom, E.; Lindeberg, G.; Karlén, A.; Danielson, U. H.; Sandström, A. *Bioorg. Med. Chem.* **2010**, *18*, 5413.
32. Lampa, A.; Ehrenberg, A. E.; Vema, A.; Åkerblom, E.; Lindeberg, G.; Danielson, U. H.; Karlén, A.; Sandström, A. *Bioorg. Med. Chem.* **2011**, *19*, 4917.
33. Dahl, G.; Sandström, A.; Åkerblom, E.; Danielson, U. H. *Antivir. Ther.* **2007**, *12*, 733.
34. Örtqvist, P.; Vema, A.; Ehrenberg, A.; Dahl, G.; Rönn, R.; Åkerblom, E.; Karlén, A.; Danielson, U. H.; Sandström, A. *Antivir. Ther.* **2010**, *15*, 841.
35. Beaulieu, P. L.; Gillard, J.; Bailey, M. D.; Boucher, C.; Duceppe, J.-S.; Simoneau, B.; Wang, X.-J.; Zhang, L.; Grozinger, K.; Houpis, I.; Farina, V.; Heimroth, H.; Krueger, T.; Schnaubelt, J. *J. Org. Chem.* **2005**, *70*, 5869.
36. Campbell, J. A.; Good, A. WO 2002/060926, 2002.
37. Raboisson, P. J. -M. B.; Belfrage, A. K. G. L.; Classon, B. O.; Lindquist, K. C.; Nilsson, K. M.; Rosenquist, Å. A. K.; Samuelsson, B. B.; Waehling, H. J. WO 2008/095999, 2008.
38. Liverton, N. J.; Holloway, M. K.; McCauley, J. A.; Rudd, M. T.; Butcher, J. W.; Carroll, S. S.; DiMuzio, J.; Fandozzi, C.; Gilbert, K. F.; Mao, S.-S.; McIntyre, C. J.; Nguyen, K. T.; Romano, J. J.; Stahlhut, M.; Wan, B.-L.; Olsen, D. B.; Vacca, J. P. *J. Am. Chem. Soc.* **2008**, *130*, 4607.
39. Dauban, P.; Dodd, R. H. *Org. Lett.* **2000**, *2*, 2327.
40. Caton, M. P. L.; Grant, M. S.; Pain, D. L.; Slack, R. *J. Chem. Soc.* **1965**, 5467.
41. Salituro, G. M.; Townsend, C. A. *J. Am. Chem. Soc.* **1990**, *112*, 760.
42. Brown, A. G.; Crimmin, M. J.; Edwards, P. D. *J. Chem. Soc., Perkin Trans. 1* **1992**, 123.
43. Netherton, M. R.; Fu, G. C. *Org. Lett.* **2001**, *3*, 4295.
44. Holloway, M. K.; Liverton, N. J.; McCauley, J. A.; Rudd, M. T.; Vacca, J. P.; Ludmerer, S. W.; Olsen, D. B. WO 2007/016441, 2007.
45. Bodanszky, M.; Bodanszky, A. *Chem. Commun.* **1967**, 591.
46. Wang, S. S.; Gisin, B. F.; Winter, D. P.; Makofske, R.; Kulesha, I. D.; Tzougraki, C.; Meienhofer, J. *J. Org. Chem.* **1977**, *42*, 1286.
47. Buckman, B.; Serebryany, V.; Beigelman, L.; Stoycheva, A. D.; Seiwert, S. D. WO 2011/041551, 2011.
48. Wang, A. X.; Scola, P. M. WO 2010/077783, 2010.
49. Britt, S. D.; Fu, J.; Parker, D. T.; Patane, M. A.; Raman, P.; Radetich, B.; Seepersaud, M.; Yifru, A.; Zheng, R.; Brandl, T.; Cottens, S.; Ehrhardt, C.; Randl, S. A.; Rigollier, P.; Schiering, N.; Simic, O. WO 2008/101665, 2008.
50. Schiering, N.; D Arcy, A.; Villard, F.; Simic, O.; Kamke, M.; Monnet, G.; Hassiepen, U.; Svergun, D. I.; Pulfer, R.; Eder, J.; Raman, P.; Bodendorf, U. *PNAS* **2011**, *108*, 21052.
51. Bartels-Keith, J. R.; Cieciuch, R. F. W. *Can. J. Chem.* **1968**, *46*, 2593.
52. Poliakov, A.; Hubatsch, I.; Shuman, C. F.; Stenberg, G.; Danielson, U. H. *Protein Exp. Purif.* **2002**, *25*, 363.
53. Lohmann, V.; Korner, F.; Koch, J. O.; Herian, U.; Theilmann, L.; Bartenschlager, R. *Science* **1999**, *285*, 110.
54. Comer, J. E. A. In *Drug Bioavailability: Estimation of Solubility, Permeability, Absorption and Bioavailability. Methods and Principles in Medicinal Chemistry*; Waterbeemd, H., Lennernäs, H., Artursson, P., Eds.; ; Wiley-VCH: Weinheim, 2003; Vol. 18, pp 21–45.
55. Houston, J. B. *Biochem. Pharmacol.* **1994**, *47*, 1469.
56. Obach, R. S. *Drug Metab. Dispos.* **1999**, *27*, 1350.
57. Hubatsch, I.; Ragnarsson, E. G. E.; Artursson, P. *Nat. Protoc.* **2007**, *2*, 2111.
58. Galia, E.; Nicolaides, E.; Hörter, D.; Löbenberg, R.; Reppas, C.; Dressman, J. B. *Pharm. Res.* **1998**, *15*, 698.
59. Neuhoff, S.; Artursson, P.; Zamora, I.; Ungell, A.-L. *Pharm. Res.* **2006**, *23*, 350.
60. Bergström, C. A. S.; Strafford, M.; Lazorova, L.; Avdeef, A.; Luthman, K.; Artursson, P. *J. Med. Chem.* **2003**, *46*, 558.
61. Rönn, R.; Lampa, A.; Peterson, S. D.; Gossas, T.; Åkerblom, E.; Danielson, U. H.; Karlén, A.; Sandström, A. *Bioorg. Med. Chem.* **2008**, *16*, 2955.
62. Hong, S. H.; Sanders, D. P.; Lee, C. W.; Grubbs, R. H. *J. Am. Chem. Soc.* **2005**, *127*, 17160.
63. Vermehren, J.; Sarrazin, C. *Best Pract. Res. Clin. Gastroenterol.* **2012**, *26*, 487.
64. Lampa, A. K.; Bergman, S. M.; Gustafsson, S. S.; Alogheli, H.; Åkerblom, E. B.; Lindeberg, G. G.; Svensson, R. M.; Artursson, P.; Danielson, U. H.; Karlén, A.; Sandström, A. *ACS Med. Chem. Lett.* **2014**, *5*, 249.
65. Johansson, A.; Poliakov, A.; Åkerblom, E.; Lindeberg, G.; Winiwarter, S.; Samuelsson, B.; Danielson, U. H.; Hallberg, A. *Bioorg. Med. Chem.* **2002**, *10*, 3915.
66. McMartin, C.; Bohacek, R. S. *J. Comput. Aided Mol. Des.* **1997**, *11*, 333.